Journal of the Mechanical Behavior of Biomedical Materials Physiochemical effects of acid exposure on bone composition and function --Manuscript Draft--

Manuscript Number:	JMBBM-D-22-01409R2
Article Type:	Research Paper
Section/Category:	Hard Tissues
Keywords:	Acidosis; Physiochemical; Bone composition; Biomechanics; Bone mineral
Corresponding Author:	Alix Deymier UConn Health UNITED STATES
First Author:	Margaret Easson
Order of Authors:	Margaret Easson
	Stephanie Wong
	Mikayla Moody
	Tannin A. Schmidt
	Alix Deymier
Abstract:	Bone is primarily composed of collagen and apatite, two materials which exhibit a high sensitivity to pH dysregulation. As a result, acid exposure of bone, both clinically and in the laboratory, is expected to cause compositional and mechanical changes to the tissue. Clinically, metabolic acidosis (MA), a condition characterized by a reduced physiological pH, has been shown to have negative implications on bone health, including a decrease in bone mineral density and volume as well as increased fracture risk. The addition of bone-like apatite to ionic solutions such as phosphate buffered saline (PBS) and media has been shown to acidify the solution leading to bone acid exposure. Therefore, is it essential to understand how reduced pH physiochemically affects bone composition and in turn its mechanical properties. This study investigates the specific changes in bone due to physiochemical dissolution in acid. Excised murine bones were placed in PBS solutions at different pHs: a homeostatic pH level (pH 7.4), an acidosis equivalent (pH 7.0), and an extreme acidic solution (pH 5.5). After 5 days, the bones were removed from the solutions and characterized to determine compositional and material changes. We found that bones, without cells, were able to regulate pH via buffering, leading to a decrease in bone mineral content and an increase in collagen denaturation. Both of these compositional changes contributed to an increase in bone toughness by creating a more ductile bone surface, likely preventing crack propagation. Therefore, we conclude that the skeletal systems' physiochemical response to acid exposure includes multifaceted and spatially variable compositional changes that affect bone mechanics.
Suggested Reviewers:	Markus J. Buehler Professor, Massachusetts Institute of Technology mbuehler@mit.edu He is an expert in the field and focuses on how proteins define the body.
	David A. Bushinsky Professor, University of Rochester School of Medicine and Dentistry David_bushinsky@urmc.rochester.edu He is an expert in this field and has written several papers on the impacts of acidosis.
	Jeffrey A Kraut Professor, University of California Los Angeles jkraut@ucla.edu He is an expert in the field and focuses on impacts of acidosis.
Response to Reviewers:	Response to Reviewer: Reviewer #2: Thank you for submitting your contribution entitled "Physiochemical

effects of acid exposure on bone composition and function" to Journal of the Mechanical Behavior of Biomedical Materials. The work is interesting and the paper can be accepted for publication after minor revision is performed, but some questions should be addressed:

We thank the reviewer for taking the time to go through the manuscript and will try to address all of the concerns.

Comment 1: The micromorphology of bone after acid exposure should be additionally tested and discussed. To illustrate the effects of acid exposure on bone physiological function from a microscopic perspective.

We appreciate your comment on further investigated micromorphology of bone after acid exposure. We agree that performing microcomputed tomography on these samples could have provided some useful additional insight into the effects of acid dissolution on the bone microstructure. However, since the focus of this paper was primarily to examine correlations between composition and mechanics in response to acid exposure, we prioritized analysis with Raman spectroscopy, FTIR, and X-ray Diffraction. To do so, we had to pulverize the bones into powders meaning that we are no longer able to analyze the bone for micromorphology. That said, since the mechanical testing is being performed in 3pt bend with loading focused on the middle of the shaft we expect that the any structural contribution to the mechanics would be from the cortical bone and not from any micromorphological changes to the trabecular bone. Our macro-scale measurements suggest that the thickness of the cortical bone, average centroid, and second moment of inertia remain unchanged (Figure 2). In addition, our Raman measurement in both the interior and the exterior provide strong evidence that the mineral content is reduce with acid exposure. These data sets provide data equivalent to the macrostructural and BMD measures that would have been obtained from uCT. Unless we looked at very high resolutions, there are few other microscale structures such as porosity that could have been identified in the cortical bone using µCT. Therefore, we feel that the data presented here provides insight into how acid exposure affects bone composition and mechanics in a system with minimal changes to the cortical structure.

Comment 2: Please give an explanation on why the pH rises fastest in the first three hours (PBS pH5.5).

To replicate the in vivo environment, the bone to fluid ratio in this study is maintained such that the bone does not fully undergo dissolution and instead it reaches a point of equilibrium where the solution becomes supersaturated with apatitic ions. These values were determined thanks to our previous work with biomimetic bone apatites1,2. Once equilibrium is reached, the bone mineral undergoes a continuous process of dissolution and recrystallization as seen in the body3. The rate at which the apatite dissolves, is highly complex and has been investigated by many 4-7. This is further complicated in our experimental system since the bone structure and porosity play a role in ionic transport and dissolution rate. In the system described here, it appears that at pH 5, it takes approximately 3 hours for sufficient mineral to dissolve in other to reach an equilibrium state. Because pH 5 is the most acidic it has the highest level of dissolution resulting in the largest change in pH over time.

We added the following sentences to ensure clarity. In methods section 2.1: "Fluid volumes were selected to promote chemical equilibrium."

And in the beginning of Discussion section 4.1:

"Additionally, the change in pH 5.5 showed a rapid increase during the first few hours after which a chemical equilibrium was reached."

Comment 3: Figures need more detailed processing to improve readability.

Thank you for giving us feedback on the figures. We have saved them at higher resolution to improve the readability.

References:

- 1. Wong, S. L. & Deymier, A. C. Ceram. Int. 49, 12415-12422 (2023).
- 2.Moynahan, M. M., Wong, S. L. & Deymier, A. C. PLOS ONE 16, e0250822 (2021).
- 3. Wang, L. & Nancollas, G. H. Chemical reviews 108, 4628-4669 (2008).
- 4.Bengtsson, Å., Shchukarev, A., Persson, P. & Sjöberg, S. Geochimica et Cosmochimica Acta 73, 257-267 (2009).
- 5. Valsami-Jones, E. et al. Chemical Geology 151, 215-233 (1998).
- 6.Bushinsky, D. A. & Krieger, N. S. Kidney Int 101, 1160-1170 (2022).
- 7. Dorozhkin, S. V. World Journal of Methodology 2, 1-17 (2012).

Response to Reviewer:

Reviewer #2: Thank you for submitting your contribution entitled "Physiochemical effects of acid exposure on bone composition and function" to Journal of the Mechanical Behavior of Biomedical Materials. The work is interesting and the paper can be accepted for publication after minor revision is performed, but some questions should be addressed:

We thank the reviewer for taking the time to go through the manuscript and will try to address all of the concerns.

Comment 1: The micromorphology of bone after acid exposure should be additionally tested and discussed. To illustrate the effects of acid exposure on bone physiological function from a microscopic perspective.

We appreciate your comment on further investigated micromorphology of bone after acid exposure. We agree that performing microcomputed tomography on these samples could have provided some useful additional insight into the effects of acid dissolution on the bone microstructure. However, since the focus of this paper was primarily to examine correlations between composition and mechanics in response to acid exposure, we prioritized analysis with Raman spectroscopy, FTIR, and X-ray Diffraction. To do so, we had to pulverize the bones into powders meaning that we are no longer able to analyze the bone for micromorphology. That said, since the mechanical testing is being performed in 3pt bend with loading focused on the middle of the shaft we expect that the any structural contribution to the mechanics would be from the cortical bone and not from any micromorphological changes to the trabecular bone. Our macro-scale measurements suggest that the thickness of the cortical bone, average centroid, and second moment of inertia remain unchanged (Figure 2). In addition, our Raman measurement in both the interior and the exterior provide strong evidence that the mineral content is reduce with acid exposure. These data sets provide data equivalent to the macrostructural and BMD measures that would have been obtained from µCT. Unless we looked at very high resolutions, there are few other microscale structures such as porosity that could have been identified in the cortical bone using µCT. Therefore, we feel that the data presented here provides insight into how acid exposure affects bone composition and mechanics in a system with minimal changes to the cortical structure.

Comment 2: Please give an explanation on why the pH rises fastest in the first three hours (PBS pH5.5).

To replicate the in vivo environment, the bone to fluid ratio in this study is maintained such that the bone does not fully undergo dissolution and instead it reaches a point of equilibrium where the solution becomes supersaturated with apatitic ions. These values were determined thanks to our previous work with biomimetic bone apatites^{1,2}. Once equilibrium is reached, the bone mineral undergoes a continuous process of dissolution and recrystallization as seen in the body³. The rate at which the apatite dissolves, is highly complex and has been investigated by many ⁴⁻⁷. This is further complicated in our experimental system since the bone structure and porosity play a role in ionic transport and dissolution rate. In the system described here, it appears that at pH 5, it takes approximately 3 hours for sufficient mineral to dissolve in other to reach an equilibrium state. Because pH 5 is the most acidic it has the highest level of dissolution resulting in the largest change in pH over time.

We added the following sentences to ensure clarity. In methods section 2.1: "Fluid volumes were selected to promote chemical equilibrium."

And in the beginning of Discussion section 4.1:

"Additionally, the change in pH 5.5 showed a rapid increase during the first few hours after which a chemical equilibrium was reached."

Comment 3: Figures need more detailed processing to improve readability.

Thank you for giving us feedback on the figures. We have saved them at higher resolution to improve the readability.

References:

- 1. Wong, S. L. & Deymier, A. C. Ceram. Int. 49, 12415-12422 (2023).
- 2. Moynahan, M. M., Wong, S. L. & Deymier, A. C. PLOS ONE 16, e0250822 (2021).
- 3. Wang, L. & Nancollas, G. H. Chemical reviews 108, 4628-4669 (2008).
- 4.Bengtsson, Å., Shchukarev, A., Persson, P. & Sjöberg, S. Geochimica et Cosmochimica Acta 73, 257-267 (2009).
- 5. Valsami-Jones, E. et al. Chemical Geology 151, 215-233 (1998).
- 6. Bushinsky, D. A. & Krieger, N. S. Kidney Int 101, 1160-1170 (2022).
- 7. Dorozhkin, S. V. World Journal of Methodology 2, 1-17 (2012).

Physiochemical effects of acid exposure on bone composition and function

Margaret Easson^a, Stephanie Wong^a, Mikayla Moody^a, Tannin A. Schmidt^a, Alix Deymier^a

^a Dept of Biomedical Engineering, School of Dental Medicine, University of Connecticut Health Center, Farmington, CT, USA

Corresponding Author:

Dr. Alix Deymier Assistant Professor Dept. of Biomedical Engineering School of Dental Medicine UConn Health 263 Farmington Avenue

Mail Code: 1721

Farmington, CT 06030 Phone: 860-679- 8916

Abstract

Bone is primarily composed of collagen and apatite, two materials which exhibit a high sensitivity to pH dysregulation. As a result, acid exposure of bone, both clinically and in the laboratory is expected to cause compositional and mechanical changes to the tissue. Clinically, Metabolic acidosis (MA), a condition characterized by a reduced physiological pH, has been shown to have negative implications on bone health, including a decrease in bone mineral density and volume as well as increased fracture risk. The addition of bone-like apatite to ionic solutions such as phosphate buffered saline (PBS) and media has been shown to acidify the solution leading to bone acid exposure. Therefore, is it essential to understand how reduced pH physiochemically affects bone composition and in turn its mechanical properties. This study investigates the specific changes in bone due to physiochemical dissolution in acid. Excised murine bones were placed in PBS solutions at different pHs: a homeostatic pH level (pH 7.4), an acidosis equivalent (pH 7.0), and an extreme acidic solution (pH 5.5). After 5 days, the bones were removed from the solutions and characterized to determine compositional and material changes. We found that bones, without cells, were able to regulate pH via buffering, leading to a decrease in bone mineral content and an increase in collagen denaturation. Both of these compositional changes contributed to an increase in bone toughness by creating a more ductile bone surface and preventing crack propagation. Therefore, we conclude that the skeletal systems' physiochemical response to acid exposure includes multifaceted and spatially variable compositional changes that affect bone mechanics.

Statement of Significance

Over 2 million people in the US are affected by metabolic acidosis annually leading to compromised bone health. Although physiochemical and cell-mediated dissolution have been identified as mechanisms responsible for bone loss during acidosis, their relative contributions remain unknown. By elucidating the possible contribution of physiochemical dissolution to bone structure, composition, and mechanics during acidosis, we can start to isolate the factors that most affect bone health during this disease and tailor future improved and targeted treatments.

Key words: Acidosis, Physiochemical, Bone composition, Biomechanics, Bone mineral

Abbreviations

Metabolic acidosis, MA; Bicarbonate, HCO₃; Phosphate, PO₄³-

1. Introduction

The primary components of bone, collagen and apatite mineral, both exhibit sensitivity to low pH [1-5]. This makes bones prone to structural, compositional, and mechanical modifications during exposure to acidic environments. Clinically, conditions that cause reduced blood pH, like metabolic acidosis (MA) [6], affect approximately 2 million people in the United States annually [7-10]. In these individuals, the kidneys and lungs are no longer able to excrete sufficient acid[6], and as a result the skeletal system undergoes dissolution promoting the release of buffering ions like bicarbonate (HCO₃-) and phosphate (PO₄³⁻) [11, 12]. This results in decreased bone mineral density [13], bone volume [14], and increased skeletal defects and fracture rates [15]. Despite the growing incidence of MA, the mechanism of bone dissolution and its consequences remain relatively obscure. Studies point to a 2-part mechanism including an initial physicochemical bone dissolution resulting from the chemical interactions between protons and bioapatite followed by cell-mediated resorption prompted by acid activation of osteoclasts and [16-25]. Although there have been numerous studies examining the effects of acid on osteoclast behavior [17-22, 24, 25]; little has been done to elucidate the physiochemical contributions of acid exposure to bone response.

This is also extremely important in the laboratory environment where bones are often stored in ionic solutions like media or phosphate buffered saline solution (PBS) which may undergo acidification. Studies have shown that the addition of nanocrystalline calcium deficient apatites, similar to those seen in bone, to ionic solutions, including a variety of cell-culture media, results in solution acidification[26, 27]. This seems to stem from the release of acidic ionic species from the apatite hydrated layer [26]. Since bone mineral exhibits a similar hydrated, non-apatitic surface, it is possible that solution acidification during storage of hard skeletal tissues could be a concern.

Therefore, this study focuses on delineating the physiochemical contributions of acid exposure to bone composition and mechanics by eliminating cellular processes and exclusively examining the bone response under chemical circumstances. By exclusively examining the effect of physiochemical acid exposure on bone chemistry and its secondary effects on mechanics, we will identify the contribution of physiochemical dissolution on acid-exposed bone.

2. Methods

2.1 Ex vivo acid exposure of murine bones.

All animal experiments were approved by the UConn Health Center Institutional Animal Care and Use Committee. The tibia, fibula, radius, and ulna were excised from previously frozen 4-6-month-old CD-1 wild type mice and scraped clean of soft tissue. After dissection, the bones were weighed and one of each bone was placed in a 15 ml conical tube (Fig 1A). The bones were exposed to 10 ml of 1X Phosphate Buffered Saline (PBS) that was titrated to an initial pH (pH_i) of 5.5, 7.0 or 7.4 using HCl or NaOH for 5 days at 5°C. Fluid volumes were selected to promote chemical equilibrium. pH 7.4 is representative of physiological pH, pH 7 represents acidotic murine conditions [28], and pH 5.5 represents an acidic extreme for comparison. Controls included bones not exposed to any solution and each of the PBS solutions at the varying pH_i's without the bones. Each condition was performed in triplicate. Over the course of the 5-day exposure, pH testing was performed at 0, 1, 3 and 6 hours after exposure, and every successive 24 hours thereafter using a pH probe. After 5 days, the bones and solution solutes were separated via filter paper, the bones were weighed and both bones and solute were characterized as described in the following sections. Changes in bone mass were measured from the difference in mass before and after solution exposure.

2.2 ICPOES

One solution sample from each experimental and control condition was analyzed for compositional changes using a Perkin Elmer 7300DV Dual View Inductively Coupled Plasma – Optical Emission Spectrometer (ICP-OES). We specifically examined changes in calcium (Ca), phosphorus (P), sodium (Na), and potassium (K) before and after exposure to the bones. All samples were directly analyzed at 20x dilution. Standard quality assurance procedures were employed, including initial and continuing calibration checks and blanks, duplicate samples, preparation blanks, post digestion spiked samples, and laboratory control samples.

2.3 Evaluation of tibia-fibula bone mechanics

After 5 days of solution exposure, 3-point bend tests were performed on each tibia/fibula complex using a Biomomentum Mach-1 system. The tibia/fibula complex was placed in the 3-pt bend system with an 8 mm span such that the anterior face underwent tensile loading (Fig 3A). Testing was performed in a PBS bath at 37°C. Bones were loaded at a rate of 0.1 mm/s until failure. The forces were measured using a 25 kg load cell. Post-failure, cross sections of the tibia, were measured using calipers. Measurements were made of the width of the posterior, medial, and lateral facet, the distance between the posterior facet and the anterior tip (height), as well as the cortical thickness. These values were used to calculate the second moment of inertia and average centroid of the bone assuming that it was a triangular tube. Force, displacement, and cross-sectional data were input into custom Matlab [29] code developed in our lab to calculate structural (maximum force, yield force, stiffness and work) and material (maximum stress, resilience, modulus, toughness) mechanical properties. The stiffness of each sample was determined from the linear portion of the load-displacement curve and the modulus from the stress-strain curve. The linear portion was identified by adjusting a window of points within the load-deformation or stress-strain curve to maximize the R² value for a linear-least-squares regression of the data in the window. Yield force was taken as the force at which the curve deviated from the previously determined linear region by more than 5%. Resilience was determined from the area under the stress-strain curve up to the yield stress/strain. Toughness was measured as the total area under the stress-strain curve.

2.4 Raman

Raman spectroscopy was used to determine compositional changes in the exterior and interior of the tibia after solution exposure. For the bone exterior, 5 measurements were made on the anterior facet of the tibia starting from the distal end to the point of fracture. For the interior, six points were measured across the fracture surface: one at each point of the triangular cross-section and one between each of the two points. The measurements were taken using a Witec alpha 300 Raman Spectrometer with a 785 nm laser at a power of \sim 60 mW. A 50X long range objective was used for both the interior and exterior regions of the bones with an acquisition time of 5 x 30s. All the acquired spectra were background and cosmic ray corrected using the Witec Project 5.1 program (Fig 4A &5A).

Each spectrum was fit using Lorentzian curves to fit 8 peaks of interest: the 950, 960, and 1050 Δcm^{-1} apatitic phosphate peaks, the 1000 and 1030 Δcm^{-1} phenylalanine in collagen peak, the 1070 Δcm^{-1} carbonate in apatite peak, the 1240 and 1270 Δcm^{-1} Amide III peaks, the 1450 Δcm^{-1} CH₂ bending peak, and the 1640, 1670, and joint 1660 Δcm^{-1} amide I peaks. The peak areas were then used to calculate ratios of interest including the mineral:matrix (950+960/1000) values, the CO₃:PO₄ ratio (1070/950+960), as well as collagen structural ratios such as the 1670/1640 and 1240/1270 ratios which are indicative of

denaturation [30], the 1660/1450 that we are using as an indicator of collagen to non-collagenous protein ratios, and the 1000/1660 ratio which is indicative of sidechain organization.

2.5 *FTIR*

Fourier Transform Infrared Spectroscopy (FTIR) was used to further analyze compositional changes in the bone with solution exposure [31]. After Raman spectroscopy, the bones were placed in a vacuum desiccator for ~7 days after which each bone was separately crushed using a clean mortar and pestle. This bone powder was then analyzed using a Nicolet MAGNA 560 FTIR spectrometer in Attenuated Total Reflection mode. The FTIR spectra was then acquired at a resolution of 4 cm⁻¹ with 64 scans per pixel (Fig 4B). The spectra were analyzed using OriginLab software and focused on 3 regions of interest: the ν_2 CO₃ band, the ν_4 PO₄ band, and the amide I band. ν_2 CO₃ band was deconvolved as 3 peaks centered at 864, 872, and 880 Δ cm⁻¹ which represent the B-type, A-type, and labile carbonate positions respectively. The ν_4 PO₄ band was deconvolved as 5 peaks including the 535 Δ cm⁻¹non-apatitic HPO₄, 550 Δ cm⁻¹ apatitic HPO₄, and 560, 575, and 601 Δ cm⁻¹ apatitic PO₄ peaks. The Amide 1 peak was deconvolved into 7 peaks: 1610, 1630, 1635, 1660, 1678, 1693, and 1702 Δ cm⁻¹ to measure changes in collagen cross-linking [32].

2.6 XRD

Nanoscale structure of the bone was examined via X-ray Diffractions (XRD) using a Bruker D2 Phaser XRD system operating at 30 kV and 10 mA. Each bone powder was scanned from 20° to 60° 20 with a step size of 0.02/theta at an acquisition rate of 2s/step (Fig 6A). Spectra were compared to standards from the International Center for Diffraction Data Powder Diffraction File open database to identify the phases. Peaks were then fit using a PseudoVoigt function in the Diffrac.eva program to measure the peaks centers and integral breadth. Changes in d-spacing with exposure were calculated from the peak centers. Specifically, we used the 002 peak center location to obtain the c-axis d-spacing and the 310 peak location for the a-axis d-spacing. The crystal size and microstrain were calculated from the integral breadth using the Halder-Wagner Method [33].

2.7 Statistical Analysis

Statistical differences in the quantitative measured values were determined as a function of pH using one-way ANOVA in Minitab. Significance level of 0.05 was used for all tests. All comparisons used one-way ANOVA and Fisher tests for comparison. Data is presented as the mean with error bars representing the standard deviation unless otherwise specified in the figure caption. Correlation factors were calculated between compositional, chemical, and mechanical factors to determine the relationships between the three axes of interest (Fig S4).

3. Results

3.1 Acid exposure effects on solution composition and ion exchange

The pH of the pH_i 7.0 and 7.4 solutions remained relatively constant over the 5-day exposure only exhibiting slight pH increases compared to the control samples at later time points. However, the pH_i 5.5 solution exhibited a significant increase in pH when exposed to bone at all timepoints (Fig 1B) with a final pH of 6.31 after 5 days.

All the solutions showed an increase in calcium when exposed to bone as compared to controls. This increase was much larger at pH 5.5 (>58000 μ g/L) than at pH 7.0 or 7.4 (~19000 and 14000

μg/L,,respectively) (Fig 1C). Solution potassium levels similarly increased with bone exposure (Fig 1D). The change in amount of potassium in solution with exposure seemed to have a linear decrease as pH increased. Solution sodium levels decreased at pH_i 5.5 and 7.0 but increased at 7.4 (Fig 1E). Finally, the solution phosphorus levels increased in all solutions with exposure with similar increases at pH_i 5.5 and 7.0 but smaller changes at pH 7.4 (Fig 1F). The correlation factors for Ca, P, K, and Na as a function of pH were all large with the Na exhibiting the only positive correlation while the others were negative (-0.99, -0.66, -0.99, 0.96 for Ca, P, K, and Na, respectively.

3.2 Acid exposure effects on bone mechanics

3-point bend tests were used to determine skeletal mechanics of the tibia/fibula complex. Solution exposure had no significant effect on structural mechanical properties including stiffness, maximum force, and work-to-fracture irrespective of the solution pH (Fig. S1). Similarly, the cross-sectional area data showed that there were no significant differences for the second moment of inertia or average centroid between any of the exposed and non-exposed bones (Fig 2B-C). These data were used to calculate the material mechanical properties. We found that most of the material mechanical properties were unaffected by acid-exposure including maximum stress, modulus, and resilience (Fig 3B-D). However, toughness increased significantly by 91.6% and 91.7% for pH 7.0 and 5.5 compared to controls (Fig 3E).

Correlations between the toughness and the initial pH showed a negative correlation (-0.35, Fig S4) by which a decrease in pH lead to an increase in toughness. This increase in toughness is most strongly correlated to the mineral content (-0.67) and the width of the Amide I peak (0.54) in the bone exterior. We also see a negative correlation between toughness and apatitic HPO₄ $^{-}$ (-0.58).

Although the change in modulus as a function of pH is not significant, it does exhibit some strong positive correlations with the width of the Amide I peak in the bone interior (-0.71) and Labile carbonate contents (0.53) as well as a negative correlation with Type A carbonate (-0.50).

3.3 Acid exposure effects on bone composition

Raman spectroscopy analysis indicated that there were significant decreases in mineral-to-matrix content in both the interior and exterior of the bone between pH 7.4 and 5.5, but not relative to controls (Fig 4C). Mineral to matrix content on the exterior also showed a significant decrease between pH 7.4 and pH 7.0. This drop in mineral content was strongly positively correlated to the initial pH when considering the bone interior (0.79) but had a much weaker correlation on the bone exterior (0.35). The carbonate content of the crystals was unchanged on both the interior and exterior of the bone (Fig 4D). This is in agreement with the FTIR data that shows that there is no significant change in the location of the carbonate with solution exposure, although there is a trend towards a decrease in A-type CO₃ with decreasing pH (Fig 4E). Conversely, the FTIR data points to a loss of apatitic HPO₄ with decreasing pH with a correlation factor of 0.61, with a significant loss between control and pH 5.5 (Fig 4F).

The collagen peaks also showed significant differences with solution exposure (Fig 5A-D). The 1670/1640 peak on the exterior shows a significant increase between control and pH 5.5 and an increase between pH 7.0 and pH 5.5; this is supported by the negative correlation factor between initial pH and 1670/1640 (Fig 5D). This was accompanied by an increase in the width of the joint 1660 peak (Fig 5E). The width of the 1660 peak on the interior had a significant decrease between control and pH 7.4, and a significant increase between control and pH 5.5. On the exterior, the width of 1660 had a significant increase between control and 5.5, and a strong negative correlation with initial pH (-0.80). In addition, the 1000/1660 peak also showed a significant decrease between control, pH 7.4 and pH 7.0 versus 5.5 (Fig 5C) with a

correlation factor of 0.64. However, there was no significant change between the 1000/1450 peak (Fig S4). FTIR data examining indicators of cross-linking found no change in the 1678/1692 peak area ratios (Fig 5F).

3.4 Acid-exposure effects on bone structure

The mass of the bones remained unchanged before and after exposure in all solutions (Fig 2A). The measured cross-sectional area similarly exhibited no significant change with acid exposure over 5 days (Fig 2B-C). At the nano-scale, XRD results indicated that neither the c-axis or a-axis of the bone mineral were impacted by the exposure to acidic solution (Fig 6A-B). In addition, there was no measured change in the bone mineral crystal size nor the intrinsic microstrain (Fig 6C-D).

4. Discussion

4.1 Mineral contributions to pH buffering and ionic release

All of the measured solutions showed an increase in pH over time, with the effect having a significantly larger magnitude in the more acidic solution, pH 5.5. The increase in pH is indicative of either the release of buffering ions from the bone or the sequestration of protons on the mineral surface. Additionally, the change in pH 5.5 showed a rapid increase during the first few hours after which a chemical equilibrium was reached. The release of these buffering ions, specifically CO₃²⁻ and PO₄³⁻, from the bone mineral to neutralize acidic solutions has been well documented in other ex vivo studies using neonatal calvaria [12, 34]. The sequestration of protons by bone mineral has been suggested to occur via an exchange of surface cations including sodium (Na⁺) and potassium (K⁺) [4, 35, 36]. Similar to previous studies [35], we also measured an increase in solution K⁺ suggesting a positive ion flux away from the bone and into solution. This removal of K⁺ from the bone allows for the surface sequestration of H⁺ and increased solution pH. However, we did not measure a similar efflux of sodium from the bone. This is contrary to other in vivo and explant studies [4, 36]; however, it is in agreement with studies examining the effect of acid exposure in vitro using biomimetic mineral [37]. In both this study and [37], the exposure times are long (3-5 days) allowing for crystal maturation and dissolution/reprecipitation processes to occur [38, 39]. These processes may lead to preferential reintegration of Na⁺ into the lattice due to the lack of Ca²⁺ in the PBS solution and it similar ionic radius [40]. This lack of Ca²⁺ in PBS is one of the limitations of this study which makes it less equivalent to in vivo systems. However, this provides important information for the storage of bone tissues which is generally done in PBS. In the in vitro systems, the addition of 0.05 g of biomimetic mineral to the same solutions used here led to a rapid rise in pH, plateauing in the first hour, but with a larger magnitude of change that those seen here (~3 pH units) [37]. This suggests that physiochemical dissolution of bone mineral could be sufficient for returning pH to healthy physiological levels. However, as we know, bone and soft tissue buffers ~60% of additional protons in the body [41, 42]. This suggests that the bone structure acts to regulate the ionic release by limiting the surface area of available bone mineral.

The idea that bone is dissolved in solution is supported by the measured increase in solution calcium in this *ex vivo* experiment. Increased blood/solution calcium has been used clinically and in the laboratory as an indicator of bone dissolution [43, 44]. The calcium release into solution is significantly larger at pH 5.5 than pH 7.0 and 7.4 suggesting that less mineral is dissolved at higher pHs. However, this trend is lost upon examination of the phosphorus release into solution where the solution phosphorus level is high at all pHs. Furthermore, we believe the phosphorus will almost always be released as phosphate ions. The released Ca/P ratio is 1.97 for pH 5.5 suggesting a near stoichiometric release of calcium and phosphate

from the mineral, indicating congruent mineral dissolution [45]. However, the Ca/P ratios for pH 7.0 and 7.4 are much lower with values of 0.65 and 0.75, respectively, suggesting that phosphate ions are preferentially released from bone more than calcium at higher pHs. Due to the relatively constant mineral volume, this also suggests that ionic exchange of surface ions, known as labile or non-apatitic ions, within the hydrated amorphous layer on the bone mineral surface may be occurring [46-49]. In this study, we used FTIR to determine if apatitic or labile phosphate and carbonate were being removed from the mineral during solution exposure at low and high pHs. Although we saw no significant changes between pH groups in the change of the labile carbonate amount, we did see a significant correlation constant of 0.55. This is larger than the correlation constants seen in the Type A and B carbonate suggesting that there may preferential removal of labile carbonate compared to the lattice bound carbonates. Similarly, we expected to see differences in the labile HPO₄²- between pH levels; however, the only significant loss was from the apatitic HPO₄²⁻ at pH 5.5. Even though all samples at low and high pHs may have some ionic exchange occurring within the surface layer, this suggests that dissolution at pH 5.5 primarily removes HPO₄ from the apatite Mineral HPO₄²-loss is generally associated with mineral maturation or dissolution/reprecipitation of more hydroxyapatite like mineral [50]. These results point to a change in the mechanism of ionic release between pH 5.5 and 7.0 from congruent mineral dissolution to ionic exchange within the hydrated amorphous layer of the mineral.

Our hypothesis that the mechanism of ion release from bone is pH dependent is further supported by Raman data indicating changes in the mineral-to-matrix ratio, both on the interior and exterior of the bone. In the bone exterior, we saw that the mineral:matrix ratio decreased between 7.4 and 5.5 as well as 7.0. On the interior, we also measured a decrease between pH 7.4 and pH 5.5. These decreases relative to pH 7.4 and not the control samples suggests that the mineral content may increase at pH 7.4 as compared to control followed by a decrease as the pH decreases. The decrease in mineral at pH 5.5 is well aligned with the previous measures that indicate mineral dissolution. However, the relative increase in mineral content at pH 7.4 is unexpected. This may suggest that during solution exposure at high pH, the bone undergoes precipitation of mineral into the matrix. However, the loss of calcium and phosphate from the bone into solution suggests that this is not a case of mineral precipitating from solution. Instead, an ion exchange process may be happening at pH 7.4 that is causing the amorphous layer to mature and become more crystalline, leading to an increase in the mineral content without requiring an increase in raw mineral materials from the solution. Interestingly, similar decreases in mineral:matrix ratios on the bone interior were also seen in the *in vivo* murine models of acidosis. These decreases in mineral content have previously been assigned to increased osteoclast activity in the bone during acidosis [16, 51, 52]. However, this ex vivo data clearly shows that physiochemical effects of acid exposure are sufficient to decrease the mineral content of the bone interior. The mineral loss at both the interior and exterior of the bone suggests that solution acid can travel into the bone and cause dissolution throughout. This agrees with numerous studies showing that bone has high permeability where small molecules quickly disperse throughout the tissue [53,

Even though there was a change in mineral-to-matrix levels, there was no significant change in carbonate-to-phosphate ratios. Others have shown using $ex\ vivo$ experiments that the conditions of metabolic acidosis led to a release of carbonate from the bone resulting in carbonate depletion at the bone surface [12, 16, 55]. Similar results have also been seen using $in\ vitro$ biomimetic apatites [37]. For the $ex\ vivo$ data presented here, the lack of change in CO₃:PO₄ ratio may suggest that the carbonate and phosphate levels may be decreasing at equal rates unlike previous experiments. However, FTIR data saw no differences in any of the carbonate peaks when examining the v_2 CO₃ band, including labile, type A and

type B, at the varying pHs. This seems to support the idea that there may not be notable changes in the carbonate levels with solution exposure. However, previous experiments looking at bones in acidosis primarily saw changes in carbonate content on the bone surface [12, 55]. Since FTIR was performed on powdered bones, it represents an average of values for the exterior and interior bone. Due to the small area:volume ratio of bone, it is possible that any differences in carbonate on the bone exterior is negated by the total bone powder. However, the significant positive correlation between initial pH and labile carbonate (0.55) suggests that despite a lack of significance between groups, there may be preferential removal of carbonated apatite.

XRD is often used to correlate changes in composition, such as carbonate loss to the crystal structure [56-58]. However, we saw no change in the d-spacing of the a- and c-axis. This suggests that there is no significant change in the crystalline organization and therefore likely no significant change in crystal composition after acid exposure [59]. Investigations of acid exposure of synthetic biomimetic apatites, previously showed a decrease in the c-axis and an increase in the a-axis which is associated with the loss of B-type carbonate [37]. Here the lack of change in carbonate may explain the unchanged mineral parameters. Similarly, *in vitro* experiments showed an increase in crystal size and crystallinity with acid exposure, suggesting that the mineral underwent dissolution and reprecipitation [39, 60]. But again, no such change was seen in the bones examined here in XRD, possibly due to the use of the whole bone powders similar to FTIR. Therefore, it is possible that we may have missed small regions of change. The insignificant change in bone mass and cross-section after solution exposure suggests that the total amount of affected bone may indeed be quite small compared to the whole bone tissue. Therefore, characterization techniques requiring tissue homogenization may fail to pick up on localized or small changes.

4.2 pH impacts on collagen structure

Although mineral plays a significant role in bone's ability to regulate pH, collagen and the other organics present in bone are also pH sensitive. pH has been shown to have a critical role in controlling collagen fibrillogenisis and stability [1-3]. For example, collagen exhibits decreased interfibrillar bonding and increased denaturation in acidic pH [2, 61]. To determine if solution exposure caused increased denaturation of collagen, we examined the ratios of the 1670/1640 and the 1270/1240 Raman peak areas. Although we found that the 1270/1240 ratio remained unchanged, we saw significant increases in the 1670/1640 ratio of the bone exterior at pH 5.5 compared to both control and pH 7.0. A negative correlation (-0.54) between 1670/1640 and pH suggests that exposure of the bone to acidic conditions causes significant local collagen denaturation at the bone surface especially in terms of changes to the amide I environment [62]. This is further confirmed by examination of the width of the blended 1660 peak, which shows a significant increase compared to control at pH 5.5 on both the exterior and interior, as well as a decrease in width between control and pH 7.4. Increased width points to a less ordered amide I environment likely caused by collagen denaturation and amorphization. In addition, there was a significant decrease in the 1000/1660 ratio which represents the relative levels of collagen phenylalanine to amide I. Beyond denaturation, we were interested in determining whether the bone underwent any significant changes in cross-linking with solution exposure. Using the amide I band in FTIR, we were able to examine the relative levels of non-enzymatic crosslinks in collagen as a function of solution pH. Using the area ratio of the 1678 and 1692 peaks we showed that there was a slight, but not statistically significant decrease in the ratio from control to 5.5. This suggests that physiochemical exposure to acidic solutions causes localized collagen denaturation without inducing significant non-enzymatic cross-linking. The 1660/1450 ratio also shows a significant increase from control, pH 7.4 and pH 7.0 versus pH 5.5. This could be indicative of a decrease in non-collagenous proteins relative to the collagen content.

4.3 Mechanical changes in bone

With both changes in mineral content and collagen structure, we expected there to be significant changes in the bone's mechanical properties as well. The 3-point bend tests performed on the tibias showed a significant increase in toughness at both pH 7.0 and 5.5 as compared to control. Toughness is defined as energy absorbed by a material before failure and can be controlled by numerous compositional and structural factors. The correlation analysis indicates that changes in bone toughness after solution exposure were most greatly affects by change in mineral:matrix ratios (C=-0.67). The mineral to matrix ratio is shown to decrease with reduced pH suggesting preferential dissolution of the mineral component of bone (Fig 4C). The contribution of mineral concentration to toughness is complex and hierarchical [63]. The addition of mineral to collagen structures has been associated with an increase in toughness at the nanoscale [64]. However, at larger scales, increased mineral content has been associated with decreased toughness especially in pathological systems [65]. Most relevant to the data presented here is extensive research examining low mineral-containing antler, which has shown that a decrease in mineral content relative to the organic matrix leads to an increase in tissue toughness [63, 66, 67]. An increased relative organic content allows the bone to more efficiently undergo plastic deformation and microcracking that provide intrinsic mechanisms for inhibiting crack propagation and increasing toughness. Interestingly, although the interior mineral:matrix ratio is more strongly correlated to pH than the exterior, the toughness is much more strongly correlated with the exterior mineral:matrix ratio. This suggests that mineral loss on the bone surface has significantly more impact on the bone toughness than any changes to the bone interior. Under bending, we expect that the crack will initiate on the surface under tension. A reduction in mineral content at this surface could increase the ductility of the material and blunt the crack tip inhibiting propagation.

The bone toughness is also strongly correlated with the width of the 1660 peak on the bone exterior (C=0.54). We find that the exterior 1660 peak width significantly increases with reduced pH. Since increasing peak width is an indicator of reduced molecular order this points to acid exposure having a significant effect on the collagen structure and organization especially with respect to Amide I. Such a reduction in the collagen molecular order could cause an increase in collagen energy absorption resulting increased toughness [68, 69]. However, denaturation of collagen, as measured from the ratio of the 1670/1640 peaks, is generally correlated with a decrease in toughness [62, 70, 71]. This suggests that broadening of the 1660 amide I peak and relative ratios of the 1670/1640 peaks do not necessarily represent the same changes to the collagen molecular structure. That may explain the lack of correlation between the 1670/1640 peak ratios and the 1660 peak width. Additionally, collagen cross-linking has been associated with an increase in bone toughness [72, 73]. Although increased cross-linking could have provided an explanation for the increased toughness, we saw no change in cross-linking at any pH in FTIR. Therefore, it is most likely that changes in the molecular organization of the collagen, especially in terms of the amide I organization is contributing to crack arrest and increased toughness.

Together these results suggest that acid induced loss of bone mineral accompanied by a change in collagen molecular order at the bone surface are primarily responsible for the decrease in toughness seen in the bone.

Limitations:

Although we aimed to develop an experimental setting with appropriate controls to isolate the chemical effects of acidosis on bone, there are always limitations to such simplified experiments. To start, although we selected PBS as a representation of body fluid/storage medium, the lack of calcium and certain other ions as well as proteins in the solution makes it an imperfect representation of serum. However, true equivalents of body fluid, such as simulated body fluid (SBF), would not have been appropriate as they are supersaturated and would have led to the independent precipitation of crystals [74]. The addition of proteins would have been required to avoid complex precipitation issues, which would have taken away from the goal of measuring purely ionic chemical processes.

Similarly, a pH of 5.5 is not physiological but was used here to accelerate the bone response and represent an extreme situation. The value of 5.5 was selected as it represents the absolute lowest physiological pH value seen in hypoxic tumor environments[75, 76]. With this said, this model is used to investigate changes in the bone with no cells. This simple environment of PBS with differing pH's allows us to investigate specific variables. This paper will help with further investigations of acidosis and bone, as it shows strictly what changes without cells present. Furthermore, the results can offer further analysis and confirmation of what occurs in the *in vivo* models.

In addition, although experiments were run in sealed tubes, the environment was not truly closed. The difficulty in working with a CO_2 free environment made this prohibitive. However, the rate of CO_2 uptake by water is relatively slow, time with the tube open was short, and the headspace was maintained small; therefore, we do not expect significant contributions from the atmospheric CO_2 [77].

Finally, the results shown here clearly show that the effects of acid exposure are significantly different in the bulk and on the surface of the bones. This resulted in varying results in Raman spectroscopy where the two regions were measured independently. However, for XRD and FTIR, the bones were crushed into fine powders as required by the lab techniques. Due to this processing and the small surface area/volume ratio of the tissues, it is possible that any surface variations were lost when mixed with the less affects bone interior. In the future, the use of surface specific techniques such as surface grazing XRD could be used to differentiate internal and external effects.

Conclusion:

As a composite structure composed of two pH sensitive materials bone is prone to chemical and mechanical modifications upon acid exposure both in vivo and in vitro. Here, we present data describing the compositional, structural, and mechanical consequences of physiochemical dissolution via acid exposure of *ex vivo* acellular bone. We found that in the absence of cells, bones were able to release buffering ions, sequester protons, and regulate pH. However, this led to a decrease in whole bone mineral content and an increase in collagen denaturation. Although the elastic properties of the bones remained unaffected by changes in pH, the bone toughness was significantly increased with acid exposure. Correlation studies suggest that the increased toughness is caused by a decrease in surface mineral content as well as increased collagen disorder in response to acid exposure. In conclusion, we found that the physiochemical effects of pH dysregulation on bone resulted in significant compositional changes across the bone material resulting in significant mechanical consequences.

Acknowledgments:

We would like to acknowledge the following individuals and programs: Paige Woods for assistance with the mechanical testing. We would also like to acknowledge the UConn Institute of Materials Science for the use of the XRD and FTIR systems. The UConn Center for Environmental Science and Engineering

provided the ICP-OES data. Funding was provided by Dr. Deymier's startup funds and NSF CAREER grant #2044870 as well as Dr. Schmidt's UConn Health startup funds.

Supplementary Materials

Supplementary material associated with this article can found here, _____.

Reference List

- [1] T. Hayashi, Y. Nagai, Effect of pH on the stability of collagen molecule in solution, Journal of biochemistry 73(5) (1973) 999-1006.
- [2] A.E. Russell, Effect of pH on thermal stability of collagen in the dispersed and aggregated states, Biochemical Journal 139(1) (1974) 277.
- [3] Y. Li, A. Asadi, M.R. Monroe, E.P. Douglas, pH effects on collagen fibrillogenesis in vitro: Electrostatic interactions and phosphate binding, Materials Science and Engineering: C 29(5) (2009) 1643-1649.
- [4] D.A. Bushinsky, W. Wolbach, N.E. Sessler, R. Mogilevsky, R. Levi-Setti, Physicochemical effects of acidosis on bone calcium flux and surface ion composition, Journal of Bone and Mineral Research 8(1) (1993) 93-102.
- [5] C.R. Hankermeyer, K.L. Ohashi, D.C. Delaney, J. Ross, B.R. Constantz, Dissolution rates of carbonated hydroxyapatite in hydrochloric acid, Biomaterials 23(3) (2002) 743-750.
- [6] J.A. Kraut, N.E. Madias, Metabolic acidosis: pathophysiology, diagnosis and management, Nature Reviews Nephrology 6(5) (2010) 274-285.
- [7] L. Frassetto, A. Sebastian, Age and Systemic Acid-Base Equilibrium: Analysis of Published Data, The Journals of Gerontology: Series A 51A(1) (1996) B91-B99.
- [8] A.G. Bergqvist, J.I. Schall, V.A. Stallings, B.S. Zemel, Progressive bone mineral content loss in children with intractable epilepsy treated with the ketogenic diet, The American journal of clinical nutrition 88(6) (2008) 1678-84.
- [9] L. Della Guardia, C. Roggi, H. Cena, Diet-induced acidosis and alkali supplementation, International Journal of Food Sciences and Nutrition 67(7) (2016) 754-761.
- [10] L. Frassetto, T. Banerjee, N. Powe, A. Sebastian, Acid Balance, Dietary Acid Load, and Bone Effects-A Controversial Subject, Nutrients 10(4) (2018) 517.
- [11] B. Wopenka, J.D. Pasteris, A mineralogical perspective on the apatite in bone, Materials Science and Engineering: C 25(2) (2005) 131-143.
- [12] D.A. Bushinsky, B.C. Lam, R. Nespeca, N.E. Sessler, M.D. Grynpas, Decreased bone carbonate content in response to metabolic, but not respiratory, acidosis, Am J Physiol 265(4 Pt 2) (1993) F530-6.
- [13] L.S. Tabatabai, S.R. Cummings, F.A. Tylavsky, D.C. Bauer, J.A. Cauley, S.B. Kritchevsky, A. Newman, E.M. Simonsick, T.B. Harris, A. Sebastian, D.E. Sellmeyer, A. Health, S. Body Composition, Arterialized venous bicarbonate is associated with lower bone mineral density and an increased rate of bone loss in older men and women, The Journal of clinical endocrinology and metabolism 100(4) (2015) 1343-1349.
- [14] J.A. Kraut, J.W. Coburn, Bone, acid, and osteoporosis, N Engl J Med 330(25) (1994) 1821-2.
- [15] D.E. Sellmeyer, K.L. Stone, A. Sebastian, S.R. Cummings, A high ratio of dietary animal to vegetable protein increases the rate of bone loss and the risk of fracture in postmenopausal women. Study of Osteoporotic Fractures Research Group, The American journal of clinical nutrition 73(1) (2001) 118-22.
- [16] N.S. Krieger, K.K. Frick, D.A. Bushinsky, Mechanism of acid-induced bone resorption, Current opinion in nephrology and hypertension 13(4) (2004) 423-436.
- [17] S.V. Ching, R.W. Norrdin, M.J. Fettman, R.A. LeCouteur, Trabecular bone remodeling and bone mineral density in the adult cat during chronic dietary acidification with ammonium chloride, J Bone Miner Res 5(6) (1990) 547-56.
- [18] F.-L. Yuan, M.-H. Xu, X. Li, H. Xinlong, W. Fang, J. Dong, The Roles of Acidosis in Osteoclast Biology, Frontiers in Physiology 7(222) (2016).
- [19] A. Carano, P.H. Schlesinger, N.A. Athanasou, S.L. Teitelbaum, H.C. Blair, Acid and base effects on avian osteoclast activity, American Journal of Physiology-Cell Physiology 264(3) (1993) C694-C701.

- [20] T.R. ARNETT, D.W. DEMPSTER, Effect of pH on bone resorption by rat osteoclasts in vitro, Endocrinology 119(1) (1986) 119-124.
- [21] T.R. Arnett, M. Spowage, Modulation of the resorptive activity of rat osteoclasts by small changes in extracellular pH near the physiological range, Bone 18(3) (1996) 277-9.
- [22] S. Meghji, M.S. Morrison, B. Henderson, T.R. Arnett, pH dependence of bone resorption: Mouse calvarial osteoclasts are activated by acidosis, American Journal of Physiology Endocrinology and Metabolism 280(1 43-1) (2001) E112-E119.
- [23] A. Jara, A.J. Felsenfeld, J. Bover, C.R. Kleeman, Chronic metabolic acidosis in azotemic rats on a high-phosphate diet halts the progression of renal disease, Kidney International 58(3) (2000) 1023-1032.
- [24] J. Assapun, N. Charoenphandhu, N. Krishnamra, Early acceleration phase and late stationary phase of remodeling imbalance in long bones of male rats exposed to long-standing acidemia: a 10-month longitudinal study using bone histomorphometry, Calcif Tissue Int 85(1) (2009) 1-9.
- [25] R.J. Murrills, L.S. Stein, D.W. Dempster, Stimulation of bone resorption and osteoclast clear zone formation by low pH: A time-course study, Journal of Cellular Physiology 154(3) (1993) 511-518.
- [26] C. Drouet, N. Vandecandelaère, A. Burger-Kentischer, I. Trick, C.G. Kohl, T. Maucher, M. Mueller, F.E. Weber, Nanocrystalline Apatites: Post-Immersion Acidification and How to Avoid It— Application to Antibacterial Bone Substitutes, Bioengineering, 2023.
- [27] J. Gustavsson, M.P. Ginebra, E. Engel, J. Planell, Ion reactivity of calcium-deficient hydroxyapatite in standard cell culture media, Acta Biomater 7(12) (2011) 4242-52.
- [28] A.K. Peterson, M. Moody, I. Nakashima, R. Abraham, T.A. Schmidt, D. Rowe, A. Deymier, Effects of acidosis on the structure, composition, and function of adult murine femurs, Acta Biomater. 121 (2021) 484-496.
- [29] MATLAB, Available at: www.mathworks.com.
- [30] C.D. Flanagan, M. Unal, O. Akkus, C.M. Rimnac, Raman spectral markers of collagen denaturation and hydration in human cortical bone tissue are affected by radiation sterilization and high cycle fatigue damage, J. Mech. Behav. Biomed. Mater. 75 (2017) 314-321.
- [31] C. Rey, O. Marsan, C. Combes, C. Drouet, D. Grossin, S. Sarda, Characterization of Calcium Phosphates Using Vibrational Spectroscopies, in: B. Ben-Nissan (Ed.), Advances in Calcium Phosphate Biomaterials, Springer, Berlin, 2014, pp. 229-266.
- [32] E.P. Paschalis, K. Verdelis, S.B. Doty, A.L. Boskey, R. Mendelsohn, M. Yamauchi, Spectroscopic characterization of collagen cross-links in bone, J Bone Miner Res 16(10) (2001) 1821-8.
- [33] D. Nath, F. Singh, R. Das, X-ray diffraction analysis by Williamson-Hall, Halder-Wagner and size-strain plot methods of CdSe nanoparticles- a comparative study, Mater. Chem. Phys. 239 (2020) 122021.
- [34] D. Bushinsky, N. Krieger, D. Geisser, E. Grossman, F. Coe, Effects of pH on bone calcium and proton fluxes in vitro, American Journal of Physiology-Renal Physiology 245(2) (1983) F204-F209.
- [35] D.A. Bushinsky, K. Gavrilov, J.M. Chabala, J.D.B. Featherstone, R. Levi-Setti, Effect of Metabolic Acidosis on the Potassium Content of Bone, Journal of Bone and Mineral Research 12(10) (1997) 1664-1671.
- [36] J.M. Burnell, Changes in bone sodium and carbonate in metabolic acidosis and alkalosis in the dog, The Journal of Clinical Investigation 50(2) (1971) 327-331.
- [37] M.M. Moynahan, S.L. Wong, A.C. Deymier, Beyond dissolution: Xerostomia rinses affect composition and structure of biomimetic dental mineral in vitro, PLOS ONE 16(4) (2021) e0250822.
- [38] N. Vandecandelaere, C. Rey, C. Drouet, Biomimetic apatite-based biomaterials: on the critical impact of synthesis and post-synthesis parameters, Journal of materials science. Materials in medicine 23(11) (2012) 2593-606.

- [39] J.M.P.M. Borggreven, F.C.M. Driessens, J.W.E. van Dijk, Dissolution and precipitation reactions in human tooth enamel under weak acid conditions, Arch. Oral Biol. 31(3) (1986) 139-144.
- [40] R. Shannon, Revised effective ionic radii and systematic studies of interatomic distances in halides and chalcogenides, Acta Crystallographica Section A 32(5) (1976) 751-767.
- [41] P.d.D.A. Bushinsky, The contribution of acidosis to renal osteodystrophy, Kidney International 47(6) (1995) 1816-1832.
- [42] R.C. Swan, R.F. Pitts, Neutralization of infused acid by nephrectomized dogs, J Clin Invest 34(2) (1955) 205-12.
- [43] A.D. Renaghan, M.H. Rosner, Hypercalcemia: etiology and management, Nephrology Dialysis Transplantation 33(4) (2018) 549-551.
- [44] W.H. Bergstrom, F.D. Ruva, Changes in bone sodium during acute acidosis in the rat, American Journal of Physiology-Legacy Content 198(5) (1960) 1126-1128.
- [45] E.D. Pellegrino, R.M. Biltz, Bone carbonate and the Ca to P molar ratio, Nature 219(5160) (1968) 1261-1262.
- [46] M. Duer, A. Veis, Bone mineralization: Water brings order, Nat Mater 12(12) (2013) 1081-2.
- [47] N.H. De Leeuw, A computer modelling study of the uptake and segregation of fluoride ions at the hydrated hydroxyapatite (0001) surface: introducing a Ca10(PO4)6(OH)2 potential model, Phys. Chem. Chem. Phys. 6 (2004) 1860.
- [48] C. Drouet, M. Aufray, S. Rollin-Martinet, N. Vandecandelaère, D. Grossin, F. Rossignol, E. Champion, A. Navrotsky, C. Rey, Nanocrystalline apatites: The fundamental role of water, American Mineralogist 103(4) (2018) 550-564.
- [49] J.R. Dorvee, A. Veis, Water in the formation of biogenic minerals: Peeling away the hydration layers, J. Struct. Biol. 183(2) (2013) 278-303.
- [50] R. Legros, N. Balmain, G. Bonel, Age-related changes in mineral of rat and bovine cortical bone, Calcif Tissue Int 41(3) (1987) 137-44.
- [51] K.K. Frick, D.A. Bushinsky, Metabolic acidosis stimulates RANKL RNA expression in bone through a cyclo-oxygenase-dependent mechanism, Journal of bone and mineral research 18(7) (2003) 1317-1325.
- [52] N.S. Krieger, D.A. Bushinsky, K.K. Frick, RENAL RESEARCH INSTITUTE SYMPOSIUM: Cellular Mechanisms of Bone Resorption Induced by Metabolic Acidosis, Seminars in Dialysis 16(6) (2003) 463-466.
- [53] T. Beno, Y.-J. Yoon, S.C. Cowin, S.P. Fritton, Estimation of bone permeability using accurate microstructural measurements, J. Biomech. 39(13) (2006) 2378-2387.
- [54] S.P. Fritton, S. Weinbaum, Fluid and solute transport in bone: flow-induced mechanotransduction, Annual review of fluid mechanics 41 (2009) 347-374.
- [55] D.A. Bushinsky, R. Levi-Setti, F.L. Coe, Ion microprobe determination of bone surface elements: effects of reduced medium pH, American Journal of Physiology-Renal Physiology 250(6) (1986) F1090-F1097.
- [56] R.Z. LeGeros, O.R. Trautz, E. Klein, J.P. LeGeros, Two types of carbonate substitution in the apatite structure, Experientia 25(1) (1969) 5-7.
- [57] A. Bigi, G. Cojazzi, S. Panzavolta, A. Ripamonti, N. Roveri, M. Romanello, K. Noris Suarez, L. Moro, Chemical and structural characterization of the mineral phase from cortical and trabecular bone, Journal of inorganic biochemistry 68(1) (1997) 45-51.
- [58] C. Yoder, J. Pasteris, K. Worcester, D. Schermerhorn, M. Sternlieb, J. Goldenberg, Z. Wilt, Dehydration and Rehydration of Carbonated Fluor- and Hydroxylapatite, Minerals (2012).
- [59] A.C. Deymier, A.K. Nair, B. Depalle, Z. Qin, K. Arcot, C. Drouet, C.H. Yoder, M.J. Buehler, S. Thomopoulos, G.M. Genin, J.D. Pasteris, Protein-free formation of bone-like apatite: New insights into the key role of carbonation, Biomaterials 127 (2017) 75-88.
- [60] S.V. Dorozhkin, Dissolution mechanism of calcium apatites in acids: A review of literature, World Journal of Methodology 2(1) (2012) 1-17.

- [61] C. Mu, D. Li, W. Lin, Y. Ding, G. Zhang, Temperature induced denaturation of collagen in acidic solution, Biopolymers 86(4) (2007) 282-7.
- [62] M. Unal, H. Jung, O. Akkus, Novel Raman Spectroscopic Biomarkers Indicate That Postyield Damage Denatures Bone's Collagen, Journal of Bone and Mineral Research 31(5) (2016) 1015-1025.
- [63] M.E. Launey, M.J. Buehler, R.O. Ritchie, On the Mechanistic Origins of Toughness in Bone, Annual Review of Materials Research 40(1) (2010) 25-53.
- [64] M.J. Buehler, Nanomechanics of collagen fibrils under varying cross-link densities: Atomicstic and continuum studies, Journal of the Mechanical Behavior of Biomedical Materials I (2008) 59-67.
- [65] D.B. Burr, Bone material properties and mineral matrix contributions to fracture risk or age in women and men, J Musculoskelet Neuronal Interact 2(3) (2002) 201-4.
- [66] D. Vashishth, K.E. Tanner, W. Bonfield, Experimental validation of a microcracking-based toughening mechanism for cortical bone, J. Biomech. 36(1) (2003) 121-124.
- [67] P. Zioupos, J.D. Currey, A.J. Sedman, An examination of the micromechanics of failure of bone and antler by acoustic emission tests and Laser Scanning Confocal Microscopy, Med Eng Phys 16(3) (1994) 203-12.
- [68] J. Alfredo Uquillas, V. Kishore, O. Akkus, Genipin Crosslinking Elevates the Strength of Electrochemically Aligned Collagen to the Level of Tendons, J. Mech. Behav. Biomed. Mater. (0). [69] A.J. Bailey, D.N. Rhodes, C.W. Cater, Irradiation-Induced Crosslinking of Collagen, Radiation Research 22(4) (1964) 606-621.
- [70] X. Wang, R.A. Bank, J.M. TeKoppele, G.B. Hubbard, K.A. Althanasiou, C.M. Agrawal, Effect of collagen denaturation on the toughness of bone, Clin Orthop Relat Res 371 (2000) 228-239.
- [71] B. Depalle, Z. Qin, S.J. Shefelbine, M.J. Buehler, Influence of cross-link structure, density and mechanical properties in the mesoscale deformation mechanisms of collagen fibrils, J. Mech. Behav. Biomed. Mater. 52 (2015) 1-13.
- [72] E.M. McNerny, B. Gong, M.D. Morris, D.H. Kohn, Bone fracture toughness and strength correlate with collagen cross-link maturity in a dose-controlled lathyrism mouse model, Journal of Bone and Mineral Research 30(3) (2015) 455-464.
- [73] F.N. Schmidt, E.A. Zimmermann, G.M. Campbell, G.E. Sroga, K. Püschel, M. Amling, S.Y. Tang, D. Vashishth, B. Busse, Assessment of collagen quality associated with non-enzymatic cross-links in human bone using Fourier-transform infrared imaging, Bone 97 (2017) 243-251.
- [74] A. Oyane, H.M. Kim, T. Furuya, T. Kokubo, T. Miyazaki, T. Nakamura, Preparation and assessment of revised simulated body fluids, J Biomed Mater Res A 65(2) (2003) 188-95.
- [75] A. Som, S. Bloch, J.E. Ippolito, S. Achilefu, Acidic extracellular pH of tumors induces octamer-binding transcription factor 4 expression in murine fibroblasts in vitro and in vivo, Scientific reports 6(1) (2016) 27803.
- [76] X. Zhang, Y. Lin, R.J. Gillies, Tumor pH and Its Measurement, Journal of Nuclear Medicine 51(8) (2010) 1167-1170.
- [77] I. Prentice, G. Farquhar, M. Fasham, M. Goulden, M. Heimann, V. Jaramillo, H. Kheshgi, C. Le Quéré, R. Scholes, D.W.R. Wallace, e. al, The carbon cycle and atmospheric carbon dioxide, 2001.

Figure Legends

- **Fig 1.** Acid exposure induces bone dissolution and ionic release resulting in increased pH. (A) Schematic of the experimental setup where ulna-radius and tibia-fibula complexes were exposed to PBS at varying initial pHs. (B) Plot of solution pH as a function of time compared to its respective control solution. (C) Change in solution calcium content pre- and post 5 days of bone exposure, (D) Change in solution potassium content pre- and post 5 days of bone exposure (E) Change in solution potassium content pre- and post 5 days of bone exposure (F) Change in solution phosphorus content pre- and post 5 days of bone exposure. * indicate p<0.05.
- Fig 2. pH did not have a significant effect on bone mass of morphology (A) Plot of percent mass change pre- and post-acid exposure. Plot of the (B) second moment of inertia and (C) average centroid of the tibia at the fracture site. bar indicates p<0.05.
- **Fig 3.** Acidosis significantly affected material mechanical properties. (A)Schematic of the steps taken for three-point bend mechanical testing. Plots of (B) max stress, (C) modulus, (D) resilience, and (E) toughness as a function of solution pH.. bar indicates p<0.05.
- **Fig 4.** Acidosis affects bone mineral content and composition. (A) Representative Raman spectra of the bone surface for the 4 conditions showing the mineral associated peaks. (B) Representative FTIR spectra of the bone for the 4 conditions showing the mineral associated peaks. (C) Plot of mineral:matrix ratios (950+960/1000 peak) area ratios) for the bone interior and exterior from Raman. (D) Plot of CO₃:PO₄ ratio (1070/960 peak) area ratio) for the bone interior and exterior from Raman. (E) Plot of the FTIR ν_2 carbonate band contributions from labile, B-type and A-type carbonate, (F) Plot of the FTIR ν_4 phosphate band contributions from non-apatitic HPO₄, apatitic HPO₄, and apatitic PO₄. bar indicates p<0.05.
- **Fig 5.** Acidosis affects bone collagen structure. (A) Representative Raman spectra of the bone surface at each conditions showing the collagen specific peaks of interest. (B) Plot of the 1660:1450 peak ratio representative of relative collagen/non-collagenous protein content from the bone interior and exterior, (C) Plot of the 1000:1660 peak ratio representative of the phenylalanine contribution to collagen from the bone interior and exterior, (D) Plot of the 1670:1450 peak ratio on interior and exterior and (E) Plot of the width of 1660 peak indicating a change in collagen order. (F) Plot of the FTIR 1678:1692 peak ratio as an indicator of non-enzymatic cross-linking. bar indicates p<0.05.
- **Fig 6.** The overall atomic order of the bone was not significantly affected by acidosis. (A) Representation XRD spectra showing the peaks of interest. XRD measurements of the (B) c-axis and (C) a-axis d-spacing were not affected by acid-exposure. Similarly, atomic order parameters such as the (D) crystal size and (E) microstrain were similarly unchanged. bar indicates p<0.05.

Physiochemical effects of acid exposure on bone composition and function

Margaret Easson^a, Stephanie Wong^a, Mikayla Moody^a, Tannin A. Schmidt^a, Alix Deymier^a

^a Dept of Biomedical Engineering, School of Dental Medicine, University of Connecticut Health Center, Farmington, CT, USA

Corresponding Author:

Dr. Alix Deymier
Assistant Professor
Dept. of Biomedical Engineering
School of Dental Medicine
UConn Health
263 Farmington Avenue

Mail Code: 1721

Farmington, CT 06030 Phone: 860-679-8916

Abstract

Bone is primarily composed of collagen and apatite, two materials which exhibit a high sensitivity to pH dysregulation. As a result, acid exposure of bone, both clinically and in the laboratory is expected to cause compositional and mechanical changes to the tissue. Clinically, Metabolic acidosis (MA), a condition characterized by a reduced physiological pH, has been shown to have negative implications on bone health, including a decrease in bone mineral density and volume as well as increased fracture risk. The addition of bone-like apatite to ionic solutions such as phosphate buffered saline (PBS) and media has been shown to acidify the solution leading to bone acid exposure. Therefore, is it essential to understand how reduced pH physiochemically affects bone composition and in turn its mechanical properties. This study investigates the specific changes in bone due to physiochemical dissolution in acid. Excised murine bones were placed in PBS solutions at different pHs: a homeostatic pH level (pH 7.4), an acidosis equivalent (pH 7.0), and an extreme acidic solution (pH 5.5). After 5 days, the bones were removed from the solutions and characterized to determine compositional and material changes. We found that bones, without cells, were able to regulate pH via buffering, leading to a decrease in bone mineral content and an increase in collagen denaturation. Both of these compositional changes contributed to an increase in bone toughness by creating a more ductile bone surface and preventing crack propagation. Therefore, we conclude that the skeletal systems' physiochemical response to acid exposure includes multifaceted and spatially variable compositional changes that affect bone mechanics.

Statement of Significance

Over 2 million people in the US are affected by metabolic acidosis annually leading to compromised bone health. Although physiochemical and cell-mediated dissolution have been identified as mechanisms responsible for bone loss during acidosis, their relative contributions remain unknown. By elucidating the possible contribution of physiochemical dissolution to bone structure, composition, and mechanics during acidosis, we can start to isolate the factors that most affect bone health during this disease and tailor future improved and targeted treatments.

Key words: Acidosis, Physiochemical, Bone composition, Biomechanics, Bone mineral

Abbreviations

Metabolic acidosis, MA; Bicarbonate, HCO₃; Phosphate, PO₄³-

1. Introduction

The primary components of bone, collagen and apatite mineral, both exhibit sensitivity to low pH [1-5]. This makes bones prone to structural, compositional, and mechanical modifications during exposure to acidic environments. Clinically, conditions that cause reduced blood pH, like metabolic acidosis (MA) [6], affect approximately 2 million people in the United States annually [7-10]. In these individuals, the kidneys and lungs are no longer able to excrete sufficient acid[6], and as a result the skeletal system undergoes dissolution promoting the release of buffering ions like bicarbonate (HCO₃-) and phosphate (PO₄³⁻) [11, 12]. This results in decreased bone mineral density [13], bone volume [14], and increased skeletal defects and fracture rates [15]. Despite the growing incidence of MA, the mechanism of bone dissolution and its consequences remain relatively obscure. Studies point to a 2-part mechanism including an initial physicochemical bone dissolution resulting from the chemical interactions between protons and bioapatite followed by cell-mediated resorption prompted by acid activation of osteoclasts and [16-25]. Although there have been numerous studies examining the effects of acid on osteoclast behavior [17-22, 24, 25]; little has been done to elucidate the physiochemical contributions of acid exposure to bone response.

This is also extremely important in the laboratory environment where bones are often stored in ionic solutions like media or phosphate buffered saline solution (PBS) which may undergo acidification. Studies have shown that the addition of nanocrystalline calcium deficient apatites, similar to those seen in bone, to ionic solutions, including a variety of cell-culture media, results in solution acidification[26, 27]. This seems to stem from the release of acidic ionic species from the apatite hydrated layer [26]. Since bone mineral exhibits a similar hydrated, non-apatitic surface, it is possible that solution acidification during storage of hard skeletal tissues could be a concern.

Therefore, this study focuses on delineating the physiochemical contributions of acid exposure to bone composition and mechanics by eliminating cellular processes and exclusively examining the bone response under chemical circumstances. By exclusively examining the effect of physiochemical acid exposure on bone chemistry and its secondary effects on mechanics, we will identify the contribution of physiochemical dissolution on acid-exposed bone.

2. Methods

2.1 Ex vivo acid exposure of murine bones.

All animal experiments were approved by the UConn Health Center Institutional Animal Care and Use Committee. The tibia, fibula, radius, and ulna were excised from previously frozen 4-6-month-old CD-1 wild type mice and scraped clean of soft tissue. After dissection, the bones were weighed and one of each bone was placed in a 15 ml conical tube (Fig 1A). The bones were exposed to 10 ml of 1X Phosphate Buffered Saline (PBS) that was titrated to an initial pH (pH_i) of 5.5, 7.0 or 7.4 using HCl or NaOH for 5 days at 5°C. Fluid volumes were selected to promote chemical equilibrium. pH 7.4 is representative of physiological pH, pH 7 represents acidotic murine conditions [28], and pH 5.5 represents an acidic extreme for comparison. Controls included bones not exposed to any solution and each of the PBS solutions at the varying pH_i's without the bones. Each condition was performed in triplicate. Over the course of the 5-day exposure, pH testing was performed at 0, 1, 3 and 6 hours after exposure, and every successive 24 hours thereafter using a pH probe. After 5 days, the bones and solution solutes were separated via filter paper, the bones were weighed and both bones and solute were characterized as described in the following sections. Changes in bone mass were measured from the difference in mass before and after solution exposure.

2.2 ICPOES

One solution sample from each experimental and control condition was analyzed for compositional changes using a Perkin Elmer 7300DV Dual View Inductively Coupled Plasma – Optical Emission Spectrometer (ICP-OES). We specifically examined changes in calcium (Ca), phosphorus (P), sodium (Na), and potassium (K) before and after exposure to the bones. All samples were directly analyzed at 20x dilution. Standard quality assurance procedures were employed, including initial and continuing calibration checks and blanks, duplicate samples, preparation blanks, post digestion spiked samples, and laboratory control samples.

2.3 Evaluation of tibia-fibula bone mechanics

After 5 days of solution exposure, 3-point bend tests were performed on each tibia/fibula complex using a Biomomentum Mach-1 system. The tibia/fibula complex was placed in the 3-pt bend system with an 8 mm span such that the anterior face underwent tensile loading (Fig 3A). Testing was performed in a PBS bath at 37°C. Bones were loaded at a rate of 0.1 mm/s until failure. The forces were measured using a 25 kg load cell. Post-failure, cross sections of the tibia, were measured using calipers. Measurements were made of the width of the posterior, medial, and lateral facet, the distance between the posterior facet and the anterior tip (height), as well as the cortical thickness. These values were used to calculate the second moment of inertia and average centroid of the bone assuming that it was a triangular tube. Force, displacement, and cross-sectional data were input into custom Matlab [29] code developed in our lab to calculate structural (maximum force, yield force, stiffness and work) and material (maximum stress, resilience, modulus, toughness) mechanical properties. The stiffness of each sample was determined from the linear portion of the load-displacement curve and the modulus from the stress-strain curve. The linear portion was identified by adjusting a window of points within the load-deformation or stress-strain curve to maximize the R² value for a linear-least-squares regression of the data in the window. Yield force was taken as the force at which the curve deviated from the previously determined linear region by more than 5%. Resilience was determined from the area under the stress-strain curve up to the yield stress/strain. Toughness was measured as the total area under the stress-strain curve.

2.4 Raman

Raman spectroscopy was used to determine compositional changes in the exterior and interior of the tibia after solution exposure. For the bone exterior, 5 measurements were made on the anterior facet of the tibia starting from the distal end to the point of fracture. For the interior, six points were measured across the fracture surface: one at each point of the triangular cross-section and one between each of the two points. The measurements were taken using a Witec alpha 300 Raman Spectrometer with a 785 nm laser at a power of \sim 60 mW. A 50X long range objective was used for both the interior and exterior regions of the bones with an acquisition time of 5 x 30s. All the acquired spectra were background and cosmic ray corrected using the Witec Project 5.1 program (Fig 4A &5A).

Each spectrum was fit using Lorentzian curves to fit 8 peaks of interest: the 950, 960, and 1050 Δcm^{-1} apatitic phosphate peaks, the 1000 and 1030 Δcm^{-1} phenylalanine in collagen peak, the 1070 Δcm^{-1} carbonate in apatite peak, the 1240 and 1270 Δcm^{-1} Amide III peaks, the 1450 Δcm^{-1} CH₂ bending peak, and the 1640, 1670, and joint 1660 Δcm^{-1} amide I peaks. The peak areas were then used to calculate ratios of interest including the mineral:matrix (950+960/1000) values, the CO₃:PO₄ ratio (1070/950+960), as well as collagen structural ratios such as the 1670/1640 and 1240/1270 ratios which are indicative of

denaturation [30], the 1660/1450 that we are using as an indicator of collagen to non-collagenous protein ratios, and the 1000/1660 ratio which is indicative of sidechain organization.

2.5 *FTIR*

Fourier Transform Infrared Spectroscopy (FTIR) was used to further analyze compositional changes in the bone with solution exposure [31]. After Raman spectroscopy, the bones were placed in a vacuum desiccator for ~7 days after which each bone was separately crushed using a clean mortar and pestle. This bone powder was then analyzed using a Nicolet MAGNA 560 FTIR spectrometer in Attenuated Total Reflection mode. The FTIR spectra was then acquired at a resolution of 4 cm⁻¹ with 64 scans per pixel (Fig 4B). The spectra were analyzed using OriginLab software and focused on 3 regions of interest: the ν_2 CO₃ band, the ν_4 PO₄ band, and the amide I band. ν_2 CO₃ band was deconvolved as 3 peaks centered at 864, 872, and 880 Δ cm⁻¹ which represent the B-type, A-type, and labile carbonate positions respectively. The ν_4 PO₄ band was deconvolved as 5 peaks including the 535 Δ cm⁻¹non-apatitic HPO₄, 550 Δ cm⁻¹ apatitic HPO₄, and 560, 575, and 601 Δ cm⁻¹ apatitic PO₄ peaks. The Amide 1 peak was deconvolved into 7 peaks: 1610, 1630, 1635, 1660, 1678, 1693, and 1702 Δ cm⁻¹ to measure changes in collagen cross-linking [32].

2.6 *XRD*

Nanoscale structure of the bone was examined via X-ray Diffractions (XRD) using a Bruker D2 Phaser XRD system operating at 30 kV and 10 mA. Each bone powder was scanned from 20° to 60° 20 with a step size of 0.02/theta at an acquisition rate of 2s/step (Fig 6A). Spectra were compared to standards from the International Center for Diffraction Data Powder Diffraction File open database to identify the phases. Peaks were then fit using a PseudoVoigt function in the Diffrac.eva program to measure the peaks centers and integral breadth. Changes in d-spacing with exposure were calculated from the peak centers. Specifically, we used the 002 peak center location to obtain the c-axis d-spacing and the 310 peak location for the a-axis d-spacing. The crystal size and microstrain were calculated from the integral breadth using the Halder-Wagner Method [33].

2.7 Statistical Analysis

Statistical differences in the quantitative measured values were determined as a function of pH using one-way ANOVA in Minitab. Significance level of 0.05 was used for all tests. All comparisons used one-way ANOVA and Fisher tests for comparison. Data is presented as the mean with error bars representing the standard deviation unless otherwise specified in the figure caption. Correlation factors were calculated between compositional, chemical, and mechanical factors to determine the relationships between the three axes of interest (Fig S4).

3. Results

3.1 Acid exposure effects on solution composition and ion exchange

The pH of the pH_i 7.0 and 7.4 solutions remained relatively constant over the 5-day exposure only exhibiting slight pH increases compared to the control samples at later time points. However, the pH_i 5.5 solution exhibited a significant increase in pH when exposed to bone at all timepoints (Fig 1B) with a final pH of 6.31 after 5 days.

All the solutions showed an increase in calcium when exposed to bone as compared to controls. This increase was much larger at pH 5.5 (>58000 μ g/L) than at pH 7.0 or 7.4 (~19000 and 14000

μg/L,,respectively) (Fig 1C). Solution potassium levels similarly increased with bone exposure (Fig 1D). The change in amount of potassium in solution with exposure seemed to have a linear decrease as pH increased. Solution sodium levels decreased at pH_i 5.5 and 7.0 but increased at 7.4 (Fig 1E). Finally, the solution phosphorus levels increased in all solutions with exposure with similar increases at pH_i 5.5 and 7.0 but smaller changes at pH 7.4 (Fig 1F). The correlation factors for Ca, P, K, and Na as a function of pH were all large with the Na exhibiting the only positive correlation while the others were negative (-0.99, -0.66, -0.99, 0.96 for Ca, P, K, and Na, respectively.

3.2 Acid exposure effects on bone mechanics

3-point bend tests were used to determine skeletal mechanics of the tibia/fibula complex. Solution exposure had no significant effect on structural mechanical properties including stiffness, maximum force, and work-to-fracture irrespective of the solution pH (Fig. S1). Similarly, the cross-sectional area data showed that there were no significant differences for the second moment of inertia or average centroid between any of the exposed and non-exposed bones (Fig 2B-C). These data were used to calculate the material mechanical properties. We found that most of the material mechanical properties were unaffected by acid-exposure including maximum stress, modulus, and resilience (Fig 3B-D). However, toughness increased significantly by 91.6% and 91.7% for pH 7.0 and 5.5 compared to controls (Fig 3E).

Correlations between the toughness and the initial pH showed a negative correlation (-0.35, Fig S4) by which a decrease in pH lead to an increase in toughness. This increase in toughness is most strongly correlated to the mineral content (-0.67) and the width of the Amide I peak (0.54) in the bone exterior. We also see a negative correlation between toughness and apatitic HPO_4^- (-0.58).

Although the change in modulus as a function of pH is not significant, it does exhibit some strong positive correlations with the width of the Amide I peak in the bone interior (-0.71) and Labile carbonate contents (0.53) as well as a negative correlation with Type A carbonate (-0.50).

3.3 Acid exposure effects on bone composition

Raman spectroscopy analysis indicated that there were significant decreases in mineral-to-matrix content in both the interior and exterior of the bone between pH 7.4 and 5.5, but not relative to controls (Fig 4C). Mineral to matrix content on the exterior also showed a significant decrease between pH 7.4 and pH 7.0. This drop in mineral content was strongly positively correlated to the initial pH when considering the bone interior (0.79) but had a much weaker correlation on the bone exterior (0.35). The carbonate content of the crystals was unchanged on both the interior and exterior of the bone (Fig 4D). This is in agreement with the FTIR data that shows that there is no significant change in the location of the carbonate with solution exposure, although there is a trend towards a decrease in A-type CO₃ with decreasing pH (Fig 4E). Conversely, the FTIR data points to a loss of apatitic HPO₄ with decreasing pH with a correlation factor of 0.61, with a significant loss between control and pH 5.5 (Fig 4F).

The collagen peaks also showed significant differences with solution exposure (Fig 5A-D). The 1670/1640 peak on the exterior shows a significant increase between control and pH 5.5 and an increase between pH 7.0 and pH 5.5; this is supported by the negative correlation factor between initial pH and 1670/1640 (Fig 5D). This was accompanied by an increase in the width of the joint 1660 peak (Fig 5E). The width of the 1660 peak on the interior had a significant decrease between control and pH 7.4, and a significant increase between control and pH 5.5. On the exterior, the width of 1660 had a significant increase between control and 5.5, and a strong negative correlation with initial pH (-0.80). In addition, the 1000/1660 peak also showed a significant decrease between control, pH 7.4 and pH 7.0 versus 5.5 (Fig 5C) with a

correlation factor of 0.64. However, there was no significant change between the 1000/1450 peak (Fig S4). FTIR data examining indicators of cross-linking found no change in the 1678/1692 peak area ratios (Fig 5F).

3.4 Acid-exposure effects on bone structure

The mass of the bones remained unchanged before and after exposure in all solutions (Fig 2A). The measured cross-sectional area similarly exhibited no significant change with acid exposure over 5 days (Fig 2B-C). At the nano-scale, XRD results indicated that neither the c-axis or a-axis of the bone mineral were impacted by the exposure to acidic solution (Fig 6A-B). In addition, there was no measured change in the bone mineral crystal size nor the intrinsic microstrain (Fig 6C-D).

4. Discussion

4.1 Mineral contributions to pH buffering and ionic release

All of the measured solutions showed an increase in pH over time, with the effect having a significantly larger magnitude in the more acidic solution, pH 5.5. The increase in pH is indicative of either the release of buffering ions from the bone or the sequestration of protons on the mineral surface. Additionally, the change in pH 5.5 showed a rapid increase during the first few hours after which a chemical equilibrium was reached. The release of these buffering ions, specifically CO₃²⁻ and PO₄³⁻, from the bone mineral to neutralize acidic solutions has been well documented in other ex vivo studies using neonatal calvaria [12, 34]. The sequestration of protons by bone mineral has been suggested to occur via an exchange of surface cations including sodium (Na⁺) and potassium (K⁺) [4, 35, 36]. Similar to previous studies [35], we also measured an increase in solution K⁺ suggesting a positive ion flux away from the bone and into solution. This removal of K⁺ from the bone allows for the surface sequestration of H⁺ and increased solution pH. However, we did not measure a similar efflux of sodium from the bone. This is contrary to other in vivo and explant studies [4, 36]; however, it is in agreement with studies examining the effect of acid exposure in vitro using biomimetic mineral [37]. In both this study and [37], the exposure times are long (3-5 days) allowing for crystal maturation and dissolution/reprecipitation processes to occur [38, 39]. These processes may lead to preferential reintegration of Na⁺ into the lattice due to the lack of Ca²⁺ in the PBS solution and it similar ionic radius [40]. This lack of Ca²⁺ in PBS is one of the limitations of this study which makes it less equivalent to in vivo systems. However, this provides important information for the storage of bone tissues which is generally done in PBS. In the in vitro systems, the addition of 0.05 g of biomimetic mineral to the same solutions used here led to a rapid rise in pH, plateauing in the first hour, but with a larger magnitude of change that those seen here (~3 pH units) [37]. This suggests that physiochemical dissolution of bone mineral could be sufficient for returning pH to healthy physiological levels. However, as we know, bone and soft tissue buffers ~60% of additional protons in the body [41, 42]. This suggests that the bone structure acts to regulate the ionic release by limiting the surface area of available bone mineral.

The idea that bone is dissolved in solution is supported by the measured increase in solution calcium in this *ex vivo* experiment. Increased blood/solution calcium has been used clinically and in the laboratory as an indicator of bone dissolution [43, 44]. The calcium release into solution is significantly larger at pH 5.5 than pH 7.0 and 7.4 suggesting that less mineral is dissolved at higher pHs. However, this trend is lost upon examination of the phosphorus release into solution where the solution phosphorus level is high at all pHs. Furthermore, we believe the phosphorus will almost always be released as phosphate ions. The released Ca/P ratio is 1.97 for pH 5.5 suggesting a near stoichiometric release of calcium and phosphate

from the mineral, indicating congruent mineral dissolution [45]. However, the Ca/P ratios for pH 7.0 and 7.4 are much lower with values of 0.65 and 0.75, respectively, suggesting that phosphate ions are preferentially released from bone more than calcium at higher pHs. Due to the relatively constant mineral volume, this also suggests that ionic exchange of surface ions, known as labile or non-apatitic ions, within the hydrated amorphous layer on the bone mineral surface may be occurring [46-49]. In this study, we used FTIR to determine if apatitic or labile phosphate and carbonate were being removed from the mineral during solution exposure at low and high pHs. Although we saw no significant changes between pH groups in the change of the labile carbonate amount, we did see a significant correlation constant of 0.55. This is larger than the correlation constants seen in the Type A and B carbonate suggesting that there may preferential removal of labile carbonate compared to the lattice bound carbonates. Similarly, we expected to see differences in the labile HPO₄²⁻ between pH levels; however, the only significant loss was from the apatitic HPO₄²⁻ at pH 5.5. Even though all samples at low and high pHs may have some ionic exchange occurring within the surface layer, this suggests that dissolution at pH 5.5 primarily removes HPO₄ from the apatite Mineral HPO₄²-loss is generally associated with mineral maturation or dissolution/reprecipitation of more hydroxyapatite like mineral [50]. These results point to a change in the mechanism of ionic release between pH 5.5 and 7.0 from congruent mineral dissolution to ionic exchange within the hydrated amorphous layer of the mineral.

Our hypothesis that the mechanism of ion release from bone is pH dependent is further supported by Raman data indicating changes in the mineral-to-matrix ratio, both on the interior and exterior of the bone. In the bone exterior, we saw that the mineral:matrix ratio decreased between 7.4 and 5.5 as well as 7.0. On the interior, we also measured a decrease between pH 7.4 and pH 5.5. These decreases relative to pH 7.4 and not the control samples suggests that the mineral content may increase at pH 7.4 as compared to control followed by a decrease as the pH decreases. The decrease in mineral at pH 5.5 is well aligned with the previous measures that indicate mineral dissolution. However, the relative increase in mineral content at pH 7.4 is unexpected. This may suggest that during solution exposure at high pH, the bone undergoes precipitation of mineral into the matrix. However, the loss of calcium and phosphate from the bone into solution suggests that this is not a case of mineral precipitating from solution. Instead, an ion exchange process may be happening at pH 7.4 that is causing the amorphous layer to mature and become more crystalline, leading to an increase in the mineral content without requiring an increase in raw mineral materials from the solution. Interestingly, similar decreases in mineral:matrix ratios on the bone interior were also seen in the *in vivo* murine models of acidosis. These decreases in mineral content have previously been assigned to increased osteoclast activity in the bone during acidosis [16, 51, 52]. However, this ex vivo data clearly shows that physiochemical effects of acid exposure are sufficient to decrease the mineral content of the bone interior. The mineral loss at both the interior and exterior of the bone suggests that solution acid can travel into the bone and cause dissolution throughout. This agrees with numerous studies showing that bone has high permeability where small molecules quickly disperse throughout the tissue [53, 541.

Even though there was a change in mineral-to-matrix levels, there was no significant change in carbonate-to-phosphate ratios. Others have shown using $ex\ vivo$ experiments that the conditions of metabolic acidosis led to a release of carbonate from the bone resulting in carbonate depletion at the bone surface [12, 16, 55]. Similar results have also been seen using $in\ vitro$ biomimetic apatites [37]. For the $ex\ vivo$ data presented here, the lack of change in CO₃:PO₄ ratio may suggest that the carbonate and phosphate levels may be decreasing at equal rates unlike previous experiments. However, FTIR data saw no differences in any of the carbonate peaks when examining the v_2 CO₃ band, including labile, type A and

type B, at the varying pHs. This seems to support the idea that there may not be notable changes in the carbonate levels with solution exposure. However, previous experiments looking at bones in acidosis primarily saw changes in carbonate content on the bone surface [12, 55]. Since FTIR was performed on powdered bones, it represents an average of values for the exterior and interior bone. Due to the small area:volume ratio of bone, it is possible that any differences in carbonate on the bone exterior is negated by the total bone powder. However, the significant positive correlation between initial pH and labile carbonate (0.55) suggests that despite a lack of significance between groups, there may be preferential removal of carbonated apatite.

XRD is often used to correlate changes in composition, such as carbonate loss to the crystal structure [56-58]. However, we saw no change in the d-spacing of the a- and c-axis. This suggests that there is no significant change in the crystalline organization and therefore likely no significant change in crystal composition after acid exposure [59]. Investigations of acid exposure of synthetic biomimetic apatites, previously showed a decrease in the c-axis and an increase in the a-axis which is associated with the loss of B-type carbonate [37]. Here the lack of change in carbonate may explain the unchanged mineral parameters. Similarly, *in vitro* experiments showed an increase in crystal size and crystallinity with acid exposure, suggesting that the mineral underwent dissolution and reprecipitation [39, 60]. But again, no such change was seen in the bones examined here in XRD, possibly due to the use of the whole bone powders similar to FTIR. Therefore, it is possible that we may have missed small regions of change. The insignificant change in bone mass and cross-section after solution exposure suggests that the total amount of affected bone may indeed be quite small compared to the whole bone tissue. Therefore, characterization techniques requiring tissue homogenization may fail to pick up on localized or small changes.

4.2 pH impacts on collagen structure

Although mineral plays a significant role in bone's ability to regulate pH, collagen and the other organics present in bone are also pH sensitive. pH has been shown to have a critical role in controlling collagen fibrillogenisis and stability [1-3]. For example, collagen exhibits decreased interfibrillar bonding and increased denaturation in acidic pH [2, 61]. To determine if solution exposure caused increased denaturation of collagen, we examined the ratios of the 1670/1640 and the 1270/1240 Raman peak areas. Although we found that the 1270/1240 ratio remained unchanged, we saw significant increases in the 1670/1640 ratio of the bone exterior at pH 5.5 compared to both control and pH 7.0. A negative correlation (-0.54) between 1670/1640 and pH suggests that exposure of the bone to acidic conditions causes significant local collagen denaturation at the bone surface especially in terms of changes to the amide I environment [62]. This is further confirmed by examination of the width of the blended 1660 peak, which shows a significant increase compared to control at pH 5.5 on both the exterior and interior, as well as a decrease in width between control and pH 7.4. Increased width points to a less ordered amide I environment likely caused by collagen denaturation and amorphization. In addition, there was a significant decrease in the 1000/1660 ratio which represents the relative levels of collagen phenylalanine to amide I. Beyond denaturation, we were interested in determining whether the bone underwent any significant changes in cross-linking with solution exposure. Using the amide I band in FTIR, we were able to examine the relative levels of non-enzymatic crosslinks in collagen as a function of solution pH. Using the area ratio of the 1678 and 1692 peaks we showed that there was a slight, but not statistically significant decrease in the ratio from control to 5.5. This suggests that physiochemical exposure to acidic solutions causes localized collagen denaturation without inducing significant non-enzymatic cross-linking. The 1660/1450 ratio also shows a

significant increase from control, pH 7.4 and pH 7.0 versus pH 5.5. This could be indicative of a decrease in non-collagenous proteins relative to the collagen content.

4.3 Mechanical changes in bone

With both changes in mineral content and collagen structure, we expected there to be significant changes in the bone's mechanical properties as well. The 3-point bend tests performed on the tibias showed a significant increase in toughness at both pH 7.0 and 5.5 as compared to control. Toughness is defined as energy absorbed by a material before failure and can be controlled by numerous compositional and structural factors. The correlation analysis indicates that changes in bone toughness after solution exposure were most greatly affects by change in mineral:matrix ratios (C=-0.67). The mineral to matrix ratio is shown to decrease with reduced pH suggesting preferential dissolution of the mineral component of bone (Fig 4C). The contribution of mineral concentration to toughness is complex and hierarchical [63]. The addition of mineral to collagen structures has been associated with an increase in toughness at the nanoscale [64]. However, at larger scales, increased mineral content has been associated with decreased toughness especially in pathological systems [65]. Most relevant to the data presented here is extensive research examining low mineral-containing antler, which has shown that a decrease in mineral content relative to the organic matrix leads to an increase in tissue toughness [63, 66, 67]. An increased relative organic content allows the bone to more efficiently undergo plastic deformation and microcracking that provide intrinsic mechanisms for inhibiting crack propagation and increasing toughness. Interestingly, although the interior mineral:matrix ratio is more strongly correlated to pH than the exterior, the toughness is much more strongly correlated with the exterior mineral:matrix ratio. This suggests that mineral loss on the bone surface has significantly more impact on the bone toughness than any changes to the bone interior. Under bending, we expect that the crack will initiate on the surface under tension. A reduction in mineral content at this surface could increase the ductility of the material and blunt the crack tip inhibiting propagation.

The bone toughness is also strongly correlated with the width of the 1660 peak on the bone exterior (C=0.54). We find that the exterior 1660 peak width significantly increases with reduced pH. Since increasing peak width is an indicator of reduced molecular order this points to acid exposure having a significant effect on the collagen structure and organization especially with respect to Amide I. Such a reduction in the collagen molecular order could cause an increase in collagen energy absorption resulting increased toughness [68, 69]. However, denaturation of collagen, as measured from the ratio of the 1670/1640 peaks, is generally correlated with a decrease in toughness [62, 70, 71]. This suggests that broadening of the 1660 amide I peak and relative ratios of the 1670/1640 peaks do not necessarily represent the same changes to the collagen molecular structure. That may explain the lack of correlation between the 1670/1640 peak ratios and the 1660 peak width. Additionally, collagen cross-linking has been associated with an increase in bone toughness [72, 73]. Although increased cross-linking could have provided an explanation for the increased toughness, we saw no change in cross-linking at any pH in FTIR. Therefore, it is most likely that changes in the molecular organization of the collagen, especially in terms of the amide I organization is contributing to crack arrest and increased toughness.

Together these results suggest that acid induced loss of bone mineral accompanied by a change in collagen molecular order at the bone surface are primarily responsible for the decrease in toughness seen in the bone.

Limitations:

Although we aimed to develop an experimental setting with appropriate controls to isolate the chemical effects of acidosis on bone, there are always limitations to such simplified experiments. To start, although we selected PBS as a representation of body fluid/storage medium, the lack of calcium and certain other ions as well as proteins in the solution makes it an imperfect representation of serum. However, true equivalents of body fluid, such as simulated body fluid (SBF), would not have been appropriate as they are supersaturated and would have led to the independent precipitation of crystals [74]. The addition of proteins would have been required to avoid complex precipitation issues, which would have taken away from the goal of measuring purely ionic chemical processes.

Similarly, a pH of 5.5 is not physiological but was used here to accelerate the bone response and represent an extreme situation. The value of 5.5 was selected as it represents the absolute lowest physiological pH value seen in hypoxic tumor environments[75, 76]. With this said, this model is used to investigate changes in the bone with no cells. This simple environment of PBS with differing pH's allows us to investigate specific variables. This paper will help with further investigations of acidosis and bone, as it shows strictly what changes without cells present. Furthermore, the results can offer further analysis and confirmation of what occurs in the *in vivo* models.

In addition, although experiments were run in sealed tubes, the environment was not truly closed. The difficulty in working with a CO_2 free environment made this prohibitive. However, the rate of CO_2 uptake by water is relatively slow, time with the tube open was short, and the headspace was maintained small; therefore, we do not expect significant contributions from the atmospheric CO_2 [77].

Finally, the results shown here clearly show that the effects of acid exposure are significantly different in the bulk and on the surface of the bones. This resulted in varying results in Raman spectroscopy where the two regions were measured independently. However, for XRD and FTIR, the bones were crushed into fine powders as required by the lab techniques. Due to this processing and the small surface area/volume ratio of the tissues, it is possible that any surface variations were lost when mixed with the less affects bone interior. In the future, the use of surface specific techniques such as surface grazing XRD could be used to differentiate internal and external effects.

Conclusion:

As a composite structure composed of two pH sensitive materials bone is prone to chemical and mechanical modifications upon acid exposure both in vivo and in vitro. Here, we present data describing the compositional, structural, and mechanical consequences of physiochemical dissolution via acid exposure of *ex vivo* acellular bone. We found that in the absence of cells, bones were able to release buffering ions, sequester protons, and regulate pH. However, this led to a decrease in whole bone mineral content and an increase in collagen denaturation. Although the elastic properties of the bones remained unaffected by changes in pH, the bone toughness was significantly increased with acid exposure. Correlation studies suggest that the increased toughness is caused by a decrease in surface mineral content as well as increased collagen disorder in response to acid exposure. In conclusion, we found that the physiochemical effects of pH dysregulation on bone resulted in significant compositional changes across the bone material resulting in significant mechanical consequences.

Acknowledgments:

We would like to acknowledge the following individuals and programs: Paige Woods for assistance with the mechanical testing. We would also like to acknowledge the UConn Institute of Materials Science for the use of the XRD and FTIR systems. The UConn Center for Environmental Science and Engineering

provided the ICP-OES data. Funding was provided by Dr. Deymier's startup funds and NSF CAREER grant #2044870 as well as Dr. Schmidt's UConn Health startup funds.

Supplementary Materials

Supplementary material associated with this article can found here, _____.

Reference List

- [1] T. Hayashi, Y. Nagai, Effect of pH on the stability of collagen molecule in solution, Journal of biochemistry 73(5) (1973) 999-1006.
- [2] A.E. Russell, Effect of pH on thermal stability of collagen in the dispersed and aggregated states, Biochemical Journal 139(1) (1974) 277.
- [3] Y. Li, A. Asadi, M.R. Monroe, E.P. Douglas, pH effects on collagen fibrillogenesis in vitro: Electrostatic interactions and phosphate binding, Materials Science and Engineering: C 29(5) (2009) 1643-1649.
- [4] D.A. Bushinsky, W. Wolbach, N.E. Sessler, R. Mogilevsky, R. Levi-Setti, Physicochemical effects of acidosis on bone calcium flux and surface ion composition, Journal of Bone and Mineral Research 8(1) (1993) 93-102.
- [5] C.R. Hankermeyer, K.L. Ohashi, D.C. Delaney, J. Ross, B.R. Constantz, Dissolution rates of carbonated hydroxyapatite in hydrochloric acid, Biomaterials 23(3) (2002) 743-750.
- [6] J.A. Kraut, N.E. Madias, Metabolic acidosis: pathophysiology, diagnosis and management, Nature Reviews Nephrology 6(5) (2010) 274-285.
- [7] L. Frassetto, A. Sebastian, Age and Systemic Acid-Base Equilibrium: Analysis of Published Data, The Journals of Gerontology: Series A 51A(1) (1996) B91-B99.
- [8] A.G. Bergqvist, J.I. Schall, V.A. Stallings, B.S. Zemel, Progressive bone mineral content loss in children with intractable epilepsy treated with the ketogenic diet, The American journal of clinical nutrition 88(6) (2008) 1678-84.
- [9] L. Della Guardia, C. Roggi, H. Cena, Diet-induced acidosis and alkali supplementation, International Journal of Food Sciences and Nutrition 67(7) (2016) 754-761.
- [10] L. Frassetto, T. Banerjee, N. Powe, A. Sebastian, Acid Balance, Dietary Acid Load, and Bone Effects-A Controversial Subject, Nutrients 10(4) (2018) 517.
- [11] B. Wopenka, J.D. Pasteris, A mineralogical perspective on the apatite in bone, Materials Science and Engineering: C 25(2) (2005) 131-143.
- [12] D.A. Bushinsky, B.C. Lam, R. Nespeca, N.E. Sessler, M.D. Grynpas, Decreased bone carbonate content in response to metabolic, but not respiratory, acidosis, Am J Physiol 265(4 Pt 2) (1993) F530-6.
- [13] L.S. Tabatabai, S.R. Cummings, F.A. Tylavsky, D.C. Bauer, J.A. Cauley, S.B. Kritchevsky, A. Newman, E.M. Simonsick, T.B. Harris, A. Sebastian, D.E. Sellmeyer, A. Health, S. Body Composition, Arterialized venous bicarbonate is associated with lower bone mineral density and an increased rate of bone loss in older men and women, The Journal of clinical endocrinology and metabolism 100(4) (2015) 1343-1349.
- [14] J.A. Kraut, J.W. Coburn, Bone, acid, and osteoporosis, N Engl J Med 330(25) (1994) 1821-2.
- [15] D.E. Sellmeyer, K.L. Stone, A. Sebastian, S.R. Cummings, A high ratio of dietary animal to vegetable protein increases the rate of bone loss and the risk of fracture in postmenopausal women. Study of Osteoporotic Fractures Research Group, The American journal of clinical nutrition 73(1) (2001) 118-22.
- [16] N.S. Krieger, K.K. Frick, D.A. Bushinsky, Mechanism of acid-induced bone resorption, Current opinion in nephrology and hypertension 13(4) (2004) 423-436.
- [17] S.V. Ching, R.W. Norrdin, M.J. Fettman, R.A. LeCouteur, Trabecular bone remodeling and bone mineral density in the adult cat during chronic dietary acidification with ammonium chloride, J Bone Miner Res 5(6) (1990) 547-56.
- [18] F.-L. Yuan, M.-H. Xu, X. Li, H. Xinlong, W. Fang, J. Dong, The Roles of Acidosis in Osteoclast Biology, Frontiers in Physiology 7(222) (2016).
- [19] A. Carano, P.H. Schlesinger, N.A. Athanasou, S.L. Teitelbaum, H.C. Blair, Acid and base effects on avian osteoclast activity, American Journal of Physiology-Cell Physiology 264(3) (1993) C694-C701.

- [20] T.R. ARNETT, D.W. DEMPSTER, Effect of pH on bone resorption by rat osteoclasts in vitro, Endocrinology 119(1) (1986) 119-124.
- [21] T.R. Arnett, M. Spowage, Modulation of the resorptive activity of rat osteoclasts by small changes in extracellular pH near the physiological range, Bone 18(3) (1996) 277-9.
- [22] S. Meghji, M.S. Morrison, B. Henderson, T.R. Arnett, pH dependence of bone resorption: Mouse calvarial osteoclasts are activated by acidosis, American Journal of Physiology Endocrinology and Metabolism 280(1 43-1) (2001) E112-E119.
- [23] A. Jara, A.J. Felsenfeld, J. Bover, C.R. Kleeman, Chronic metabolic acidosis in azotemic rats on a high-phosphate diet halts the progression of renal disease, Kidney International 58(3) (2000) 1023-1032.
- [24] J. Assapun, N. Charoenphandhu, N. Krishnamra, Early acceleration phase and late stationary phase of remodeling imbalance in long bones of male rats exposed to long-standing acidemia: a 10-month longitudinal study using bone histomorphometry, Calcif Tissue Int 85(1) (2009) 1-9.
- [25] R.J. Murrills, L.S. Stein, D.W. Dempster, Stimulation of bone resorption and osteoclast clear zone formation by low pH: A time-course study, Journal of Cellular Physiology 154(3) (1993) 511-518.
- [26] C. Drouet, N. Vandecandelaère, A. Burger-Kentischer, I. Trick, C.G. Kohl, T. Maucher, M. Mueller, F.E. Weber, Nanocrystalline Apatites: Post-Immersion Acidification and How to Avoid It— Application to Antibacterial Bone Substitutes, Bioengineering, 2023.
- [27] J. Gustavsson, M.P. Ginebra, E. Engel, J. Planell, Ion reactivity of calcium-deficient hydroxyapatite in standard cell culture media, Acta Biomater 7(12) (2011) 4242-52.
- [28] A.K. Peterson, M. Moody, I. Nakashima, R. Abraham, T.A. Schmidt, D. Rowe, A. Deymier, Effects of acidosis on the structure, composition, and function of adult murine femurs, Acta Biomater. 121 (2021) 484-496.
- [29] MATLAB, Available at: www.mathworks.com.
- [30] C.D. Flanagan, M. Unal, O. Akkus, C.M. Rimnac, Raman spectral markers of collagen denaturation and hydration in human cortical bone tissue are affected by radiation sterilization and high cycle fatigue damage, J. Mech. Behav. Biomed. Mater. 75 (2017) 314-321.
- [31] C. Rey, O. Marsan, C. Combes, C. Drouet, D. Grossin, S. Sarda, Characterization of Calcium Phosphates Using Vibrational Spectroscopies, in: B. Ben-Nissan (Ed.), Advances in Calcium Phosphate Biomaterials, Springer, Berlin, 2014, pp. 229-266.
- [32] E.P. Paschalis, K. Verdelis, S.B. Doty, A.L. Boskey, R. Mendelsohn, M. Yamauchi, Spectroscopic characterization of collagen cross-links in bone, J Bone Miner Res 16(10) (2001) 1821-8.
- [33] D. Nath, F. Singh, R. Das, X-ray diffraction analysis by Williamson-Hall, Halder-Wagner and size-strain plot methods of CdSe nanoparticles- a comparative study, Mater. Chem. Phys. 239 (2020) 122021.
- [34] D. Bushinsky, N. Krieger, D. Geisser, E. Grossman, F. Coe, Effects of pH on bone calcium and proton fluxes in vitro, American Journal of Physiology-Renal Physiology 245(2) (1983) F204-F209.
- [35] D.A. Bushinsky, K. Gavrilov, J.M. Chabala, J.D.B. Featherstone, R. Levi-Setti, Effect of Metabolic Acidosis on the Potassium Content of Bone, Journal of Bone and Mineral Research 12(10) (1997) 1664-1671.
- [36] J.M. Burnell, Changes in bone sodium and carbonate in metabolic acidosis and alkalosis in the dog, The Journal of Clinical Investigation 50(2) (1971) 327-331.
- [37] M.M. Moynahan, S.L. Wong, A.C. Deymier, Beyond dissolution: Xerostomia rinses affect composition and structure of biomimetic dental mineral in vitro, PLOS ONE 16(4) (2021) e0250822.
- [38] N. Vandecandelaere, C. Rey, C. Drouet, Biomimetic apatite-based biomaterials: on the critical impact of synthesis and post-synthesis parameters, Journal of materials science. Materials in medicine 23(11) (2012) 2593-606.

- [39] J.M.P.M. Borggreven, F.C.M. Driessens, J.W.E. van Dijk, Dissolution and precipitation reactions in human tooth enamel under weak acid conditions, Arch. Oral Biol. 31(3) (1986) 139-144.
- [40] R. Shannon, Revised effective ionic radii and systematic studies of interatomic distances in halides and chalcogenides, Acta Crystallographica Section A 32(5) (1976) 751-767.
- [41] P.d.D.A. Bushinsky, The contribution of acidosis to renal osteodystrophy, Kidney International 47(6) (1995) 1816-1832.
- [42] R.C. Swan, R.F. Pitts, Neutralization of infused acid by nephrectomized dogs, J Clin Invest 34(2) (1955) 205-12.
- [43] A.D. Renaghan, M.H. Rosner, Hypercalcemia: etiology and management, Nephrology Dialysis Transplantation 33(4) (2018) 549-551.
- [44] W.H. Bergstrom, F.D. Ruva, Changes in bone sodium during acute acidosis in the rat, American Journal of Physiology-Legacy Content 198(5) (1960) 1126-1128.
- [45] E.D. Pellegrino, R.M. Biltz, Bone carbonate and the Ca to P molar ratio, Nature 219(5160) (1968) 1261-1262.
- [46] M. Duer, A. Veis, Bone mineralization: Water brings order, Nat Mater 12(12) (2013) 1081-2.
- [47] N.H. De Leeuw, A computer modelling study of the uptake and segregation of fluoride ions at the hydrated hydroxyapatite (0001) surface: introducing a Ca10(PO4)6(OH)2 potential model, Phys. Chem. Phys. 6 (2004) 1860.
- [48] C. Drouet, M. Aufray, S. Rollin-Martinet, N. Vandecandelaère, D. Grossin, F. Rossignol, E. Champion, A. Navrotsky, C. Rey, Nanocrystalline apatites: The fundamental role of water, American Mineralogist 103(4) (2018) 550-564.
- [49] J.R. Dorvee, A. Veis, Water in the formation of biogenic minerals: Peeling away the hydration layers, J. Struct. Biol. 183(2) (2013) 278-303.
- [50] R. Legros, N. Balmain, G. Bonel, Age-related changes in mineral of rat and bovine cortical bone, Calcif Tissue Int 41(3) (1987) 137-44.
- [51] K.K. Frick, D.A. Bushinsky, Metabolic acidosis stimulates RANKL RNA expression in bone through a cyclo-oxygenase-dependent mechanism, Journal of bone and mineral research 18(7) (2003) 1317-1325.
- [52] N.S. Krieger, D.A. Bushinsky, K.K. Frick, RENAL RESEARCH INSTITUTE SYMPOSIUM: Cellular Mechanisms of Bone Resorption Induced by Metabolic Acidosis, Seminars in Dialysis 16(6) (2003) 463-466.
- [53] T. Beno, Y.-J. Yoon, S.C. Cowin, S.P. Fritton, Estimation of bone permeability using accurate microstructural measurements, J. Biomech. 39(13) (2006) 2378-2387.
- [54] S.P. Fritton, S. Weinbaum, Fluid and solute transport in bone: flow-induced mechanotransduction, Annual review of fluid mechanics 41 (2009) 347-374.
- [55] D.A. Bushinsky, R. Levi-Setti, F.L. Coe, Ion microprobe determination of bone surface elements: effects of reduced medium pH, American Journal of Physiology-Renal Physiology 250(6) (1986) F1090-F1097.
- [56] R.Z. LeGeros, O.R. Trautz, E. Klein, J.P. LeGeros, Two types of carbonate substitution in the apatite structure, Experientia 25(1) (1969) 5-7.
- [57] A. Bigi, G. Cojazzi, S. Panzavolta, A. Ripamonti, N. Roveri, M. Romanello, K. Noris Suarez, L. Moro, Chemical and structural characterization of the mineral phase from cortical and trabecular bone, Journal of inorganic biochemistry 68(1) (1997) 45-51.
- [58] C. Yoder, J. Pasteris, K. Worcester, D. Schermerhorn, M. Sternlieb, J. Goldenberg, Z. Wilt, Dehydration and Rehydration of Carbonated Fluor- and Hydroxylapatite, Minerals (2012).
- [59] A.C. Deymier, A.K. Nair, B. Depalle, Z. Qin, K. Arcot, C. Drouet, C.H. Yoder, M.J. Buehler, S. Thomopoulos, G.M. Genin, J.D. Pasteris, Protein-free formation of bone-like apatite: New insights into the key role of carbonation, Biomaterials 127 (2017) 75-88.
- [60] S.V. Dorozhkin, Dissolution mechanism of calcium apatites in acids: A review of literature, World Journal of Methodology 2(1) (2012) 1-17.

- [61] C. Mu, D. Li, W. Lin, Y. Ding, G. Zhang, Temperature induced denaturation of collagen in acidic solution, Biopolymers 86(4) (2007) 282-7.
- [62] M. Unal, H. Jung, O. Akkus, Novel Raman Spectroscopic Biomarkers Indicate That Postyield Damage Denatures Bone's Collagen, Journal of Bone and Mineral Research 31(5) (2016) 1015-1025.
- [63] M.E. Launey, M.J. Buehler, R.O. Ritchie, On the Mechanistic Origins of Toughness in Bone, Annual Review of Materials Research 40(1) (2010) 25-53.
- [64] M.J. Buehler, Nanomechanics of collagen fibrils under varying cross-link densities: Atomicstic and continuum studies, Journal of the Mechanical Behavior of Biomedical Materials I (2008) 59-67
- [65] D.B. Burr, Bone material properties and mineral matrix contributions to fracture risk or age in women and men, J Musculoskelet Neuronal Interact 2(3) (2002) 201-4.
- [66] D. Vashishth, K.E. Tanner, W. Bonfield, Experimental validation of a microcracking-based toughening mechanism for cortical bone, J. Biomech. 36(1) (2003) 121-124.
- [67] P. Zioupos, J.D. Currey, A.J. Sedman, An examination of the micromechanics of failure of bone and antler by acoustic emission tests and Laser Scanning Confocal Microscopy, Med Eng Phys 16(3) (1994) 203-12.
- [68] J. Alfredo Uquillas, V. Kishore, O. Akkus, Genipin Crosslinking Elevates the Strength of Electrochemically Aligned Collagen to the Level of Tendons, J. Mech. Behav. Biomed. Mater. (0). [69] A.J. Bailey, D.N. Rhodes, C.W. Cater, Irradiation-Induced Crosslinking of Collagen, Radiation Research 22(4) (1964) 606-621.
- [70] X. Wang, R.A. Bank, J.M. TeKoppele, G.B. Hubbard, K.A. Althanasiou, C.M. Agrawal, Effect of collagen denaturation on the toughness of bone, Clin Orthop Relat Res 371 (2000) 228-239.
- [71] B. Depalle, Z. Qin, S.J. Shefelbine, M.J. Buehler, Influence of cross-link structure, density and mechanical properties in the mesoscale deformation mechanisms of collagen fibrils, J. Mech. Behav. Biomed. Mater. 52 (2015) 1-13.
- [72] E.M. McNerny, B. Gong, M.D. Morris, D.H. Kohn, Bone fracture toughness and strength correlate with collagen cross-link maturity in a dose-controlled lathyrism mouse model, Journal of Bone and Mineral Research 30(3) (2015) 455-464.
- [73] F.N. Schmidt, E.A. Zimmermann, G.M. Campbell, G.E. Sroga, K. Püschel, M. Amling, S.Y. Tang, D. Vashishth, B. Busse, Assessment of collagen quality associated with non-enzymatic cross-links in human bone using Fourier-transform infrared imaging, Bone 97 (2017) 243-251.
- [74] A. Oyane, H.M. Kim, T. Furuya, T. Kokubo, T. Miyazaki, T. Nakamura, Preparation and assessment of revised simulated body fluids, J Biomed Mater Res A 65(2) (2003) 188-95.
- [75] A. Som, S. Bloch, J.E. Ippolito, S. Achilefu, Acidic extracellular pH of tumors induces octamer-binding transcription factor 4 expression in murine fibroblasts in vitro and in vivo, Scientific reports 6(1) (2016) 27803.
- [76] X. Zhang, Y. Lin, R.J. Gillies, Tumor pH and Its Measurement, Journal of Nuclear Medicine 51(8) (2010) 1167-1170.
- [77] I. Prentice, G. Farquhar, M. Fasham, M. Goulden, M. Heimann, V. Jaramillo, H. Kheshgi, C. Le Quéré, R. Scholes, D.W.R. Wallace, e. al, The carbon cycle and atmospheric carbon dioxide, 2001.

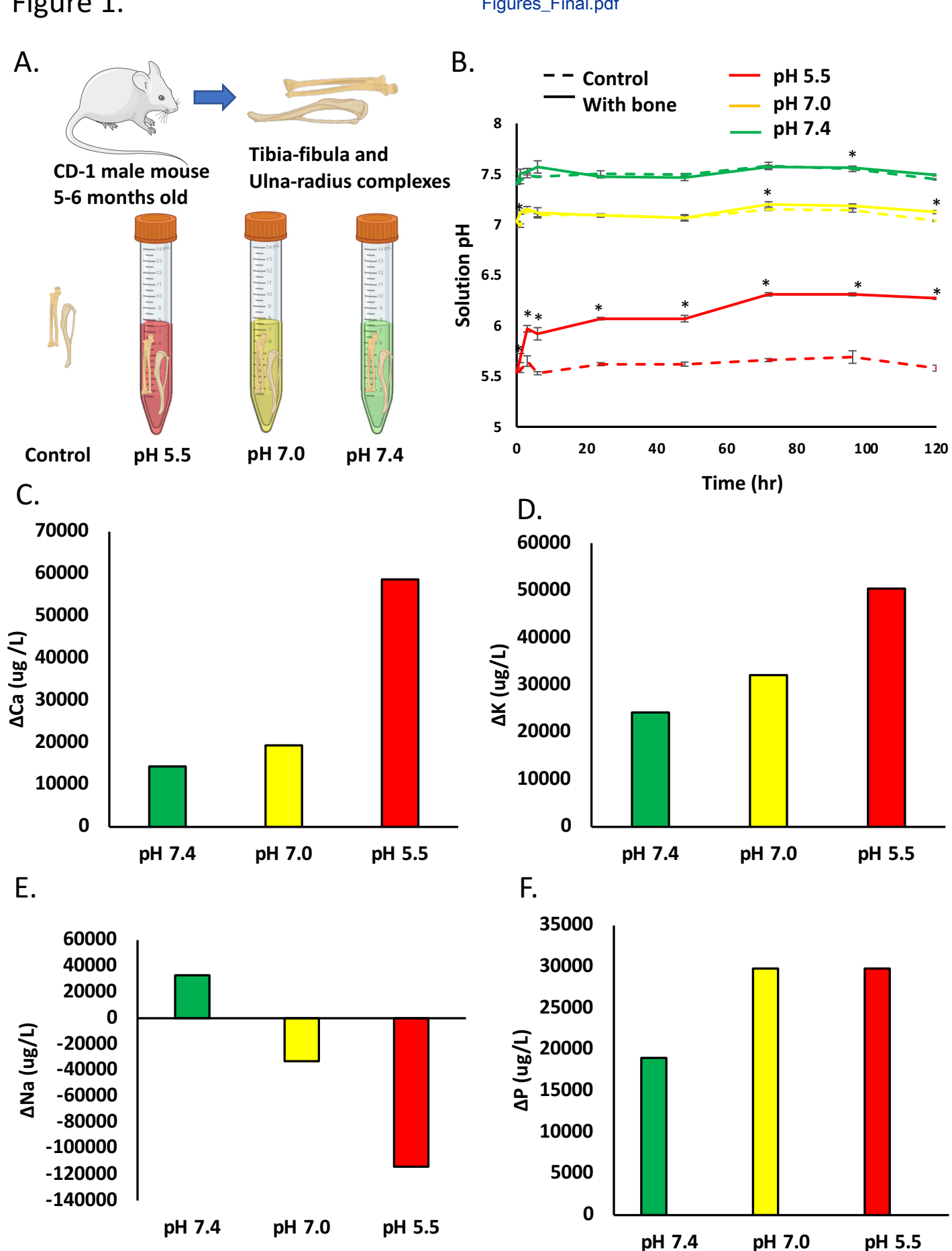
Figure Legends

- **Fig 1.** Acid exposure induces bone dissolution and ionic release resulting in increased pH. (A) Schematic of the experimental setup where ulna-radius and tibia-fibula complexes were exposed to PBS at varying initial pHs. (B) Plot of solution pH as a function of time compared to its respective control solution. (C) Change in solution calcium content pre- and post 5 days of bone exposure, (D) Change in solution potassium content pre- and post 5 days of bone exposure (E) Change in solution potassium content pre- and post 5 days of bone exposure. * indicate p<0.05.
- Fig 2. pH did not have a significant effect on bone mass of morphology (A) Plot of percent mass change pre- and post-acid exposure. Plot of the (B) second moment of inertia and (C) average centroid of the tibia at the fracture site. bar indicates p<0.05.
- **Fig 3.** Acidosis significantly affected material mechanical properties. (A)Schematic of the steps taken for three-point bend mechanical testing. Plots of (B) max stress, (C) modulus, (D) resilience, and (E) toughness as a function of solution pH.. bar indicates p<0.05.
- **Fig 4.** Acidosis affects bone mineral content and composition. (A) Representative Raman spectra of the bone surface for the 4 conditions showing the mineral associated peaks. (B) Representative FTIR spectra of the bone for the 4 conditions showing the mineral associated peaks. (C) Plot of mineral:matrix ratios (950+960/1000 peak area ratios) for the bone interior and exterior from Raman. (D) Plot of CO₃:PO₄ ratio (1070/960 peak area ratio) for the bone interior and exterior from Raman. (E) Plot of the FTIR ν_2 carbonate band contributions from labile, B-type and A-type carbonate, (F) Plot of the FTIR ν_4 phosphate band contributions from non-apatitic HPO₄, apatitic HPO₄, and apatitic PO₄. bar indicates p<0.05.
- **Fig 5.** Acidosis affects bone collagen structure. (A) Representative Raman spectra of the bone surface at each conditions showing the collagen specific peaks of interest. (B) Plot of the 1660:1450 peak ratio representative of relative collagen/non-collagenous protein content from the bone interior and exterior, (C) Plot of the 1000:1660 peak ratio representative of the phenylalanine contribution to collagen from the bone interior and exterior, (D) Plot of the 1670:1450 peak ratio on interior and exterior and (E) Plot of the width of 1660 peak indicating a change in collagen order. (F) Plot of the FTIR 1678:1692 peak ratio as an indicator of non-enzymatic cross-linking. bar indicates p<0.05.
- **Fig 6.** The overall atomic order of the bone was not significantly affected by acidosis. (A) Representation XRD spectra showing the peaks of interest. XRD measurements of the (B) c-axis and (C) a-axis d-spacing were not affected by acid-exposure. Similarly, atomic order parameters such as the (D) crystal size and (E) microstrain were similarly unchanged. bar indicates p<0.05.

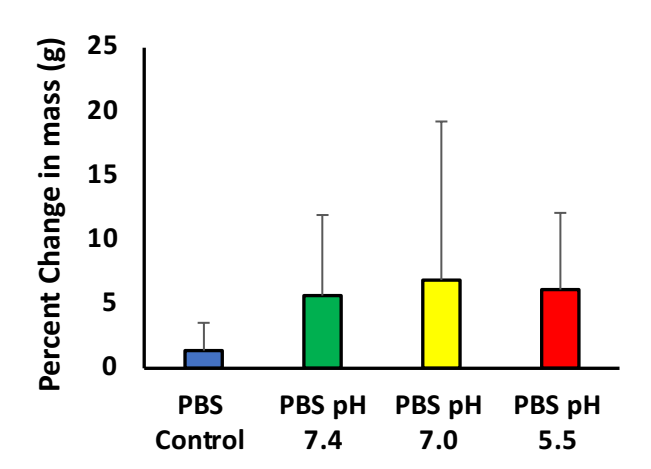
Declaration of Interest Statement

Declaration of interests

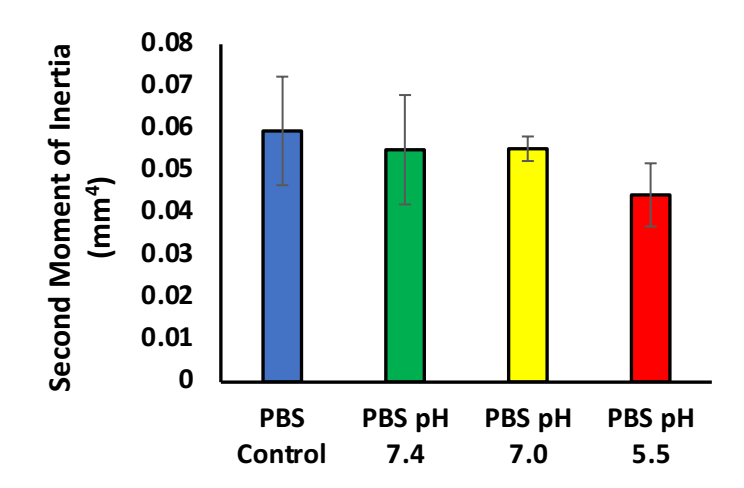
oximes The authors declare that they have no known competing financial interests or personal relationships that could have appeared to influence the work reported in this paper.
☐The authors declare the following financial interests/personal relationships which may be considered as potential competing interests:



Α.



В.



C.

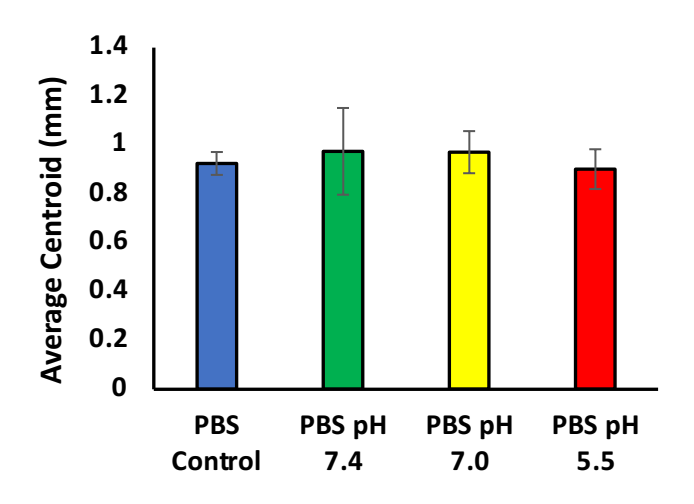


Figure 3.

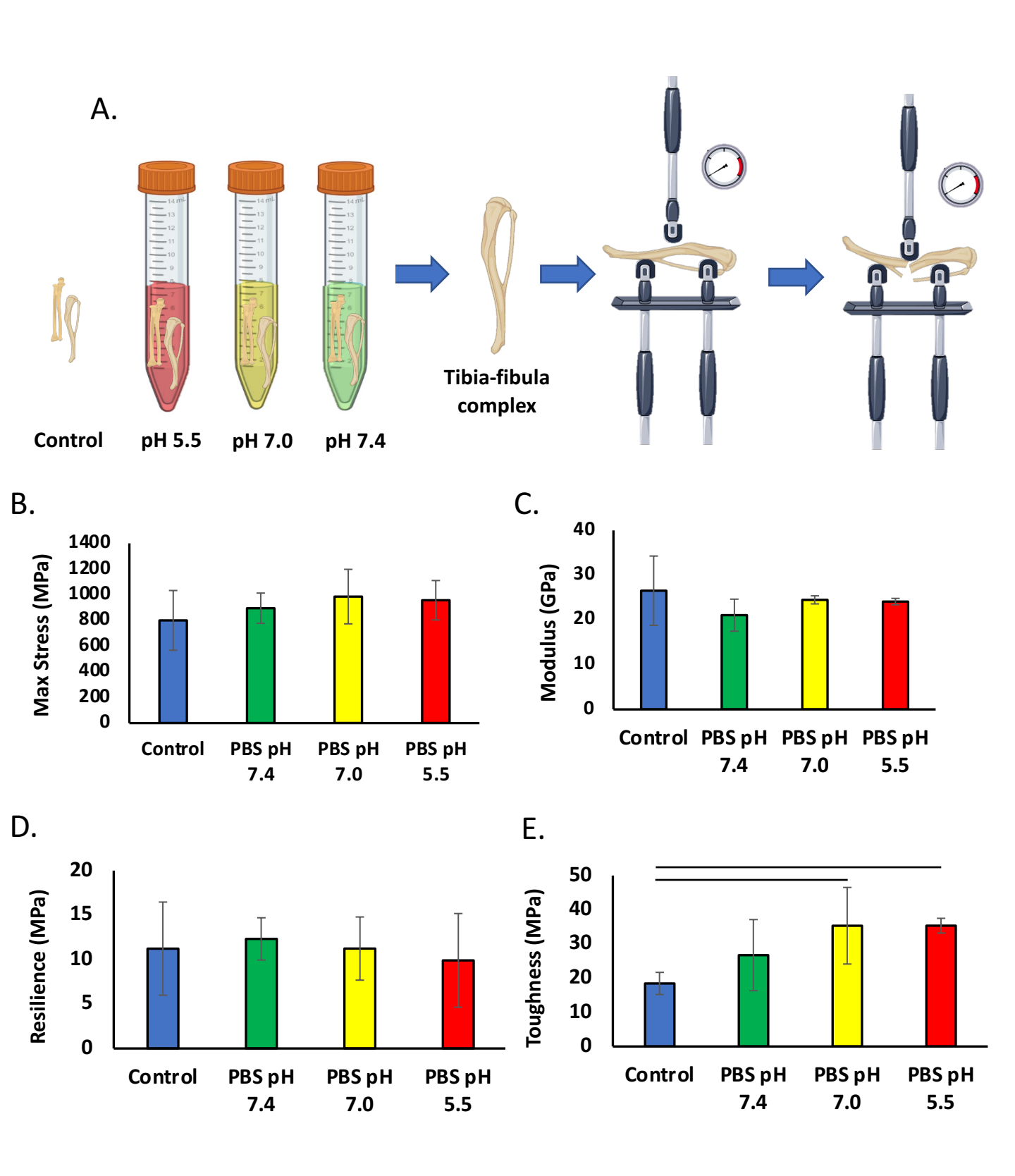


Figure 4.

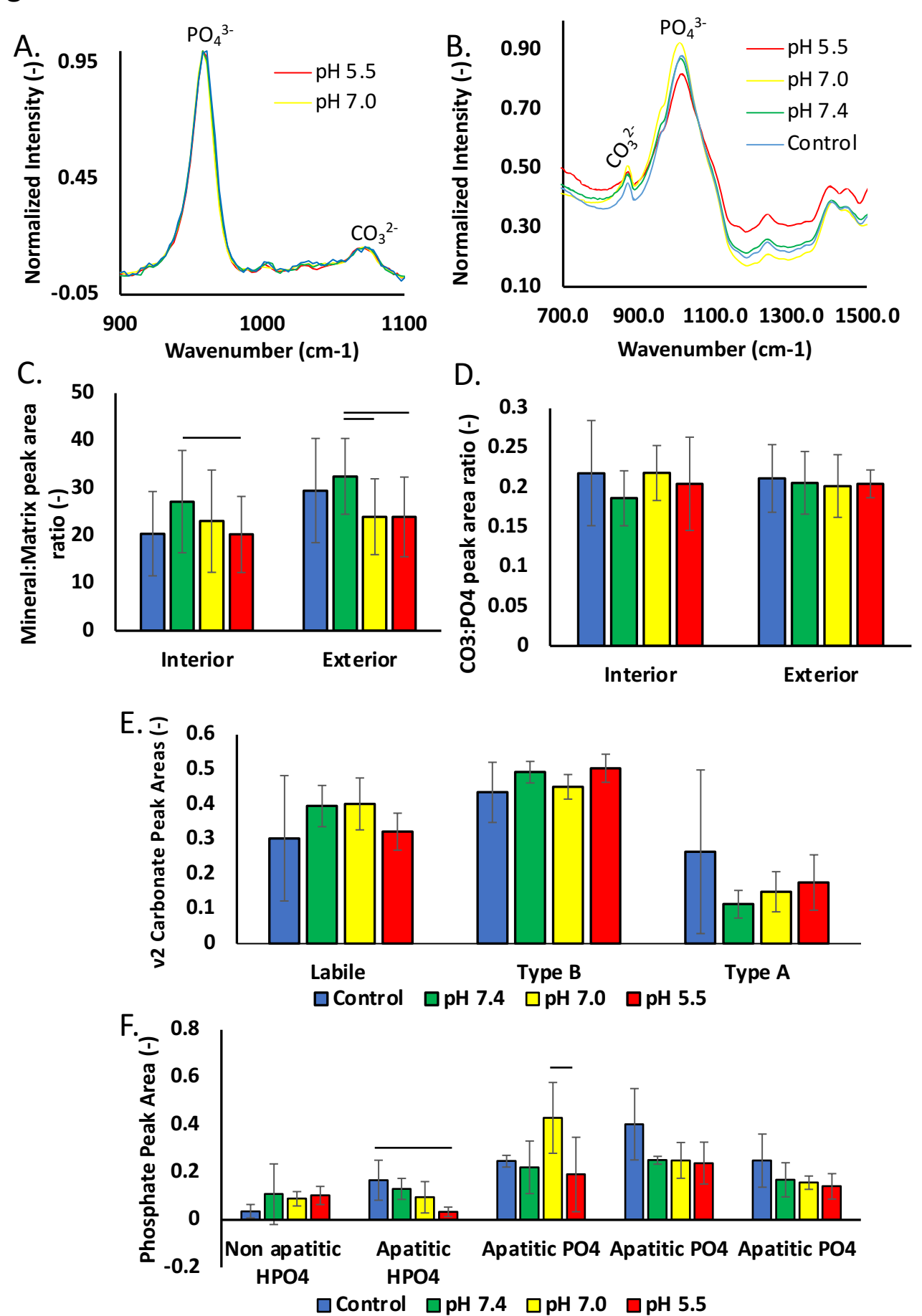


Figure 5.

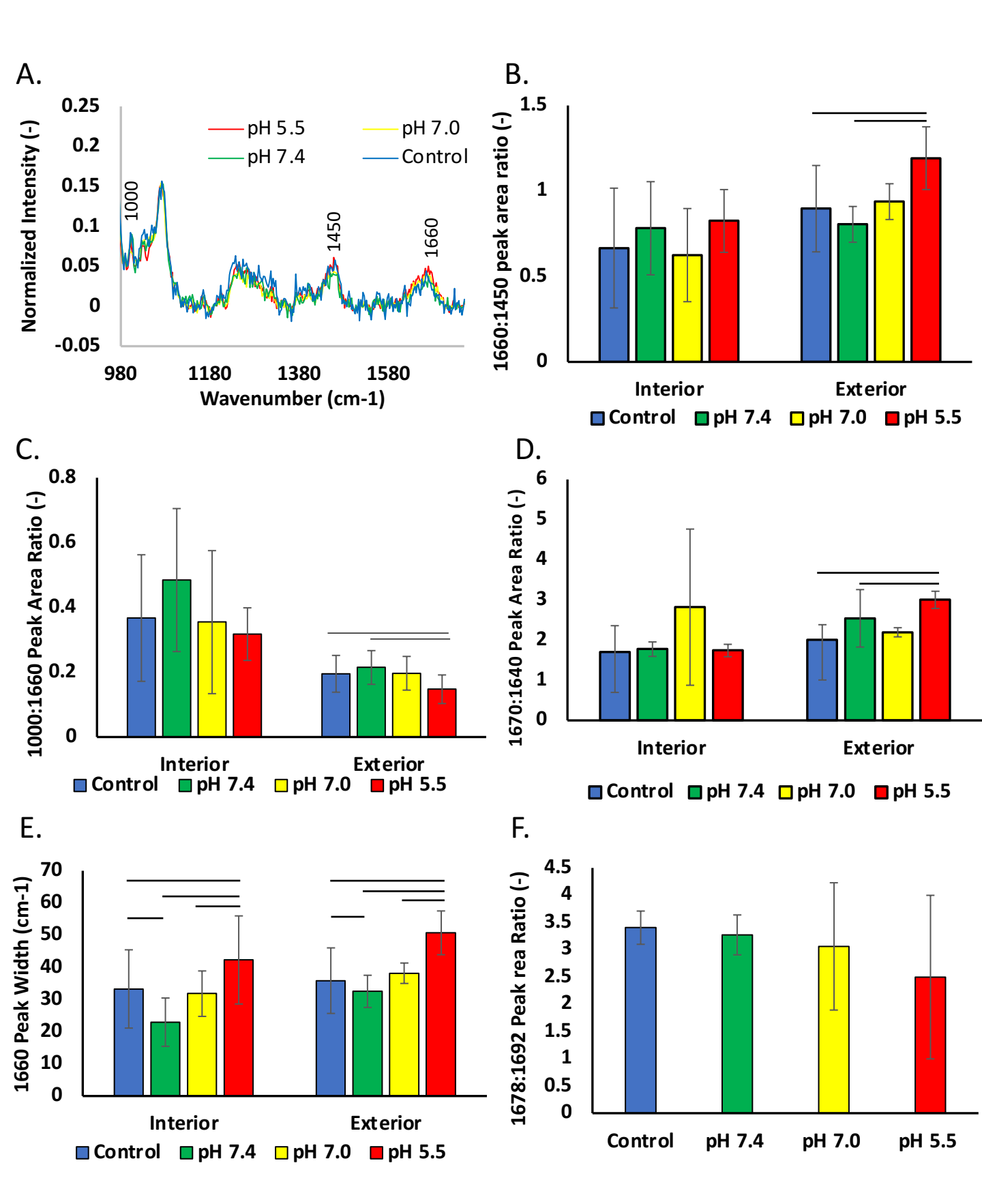
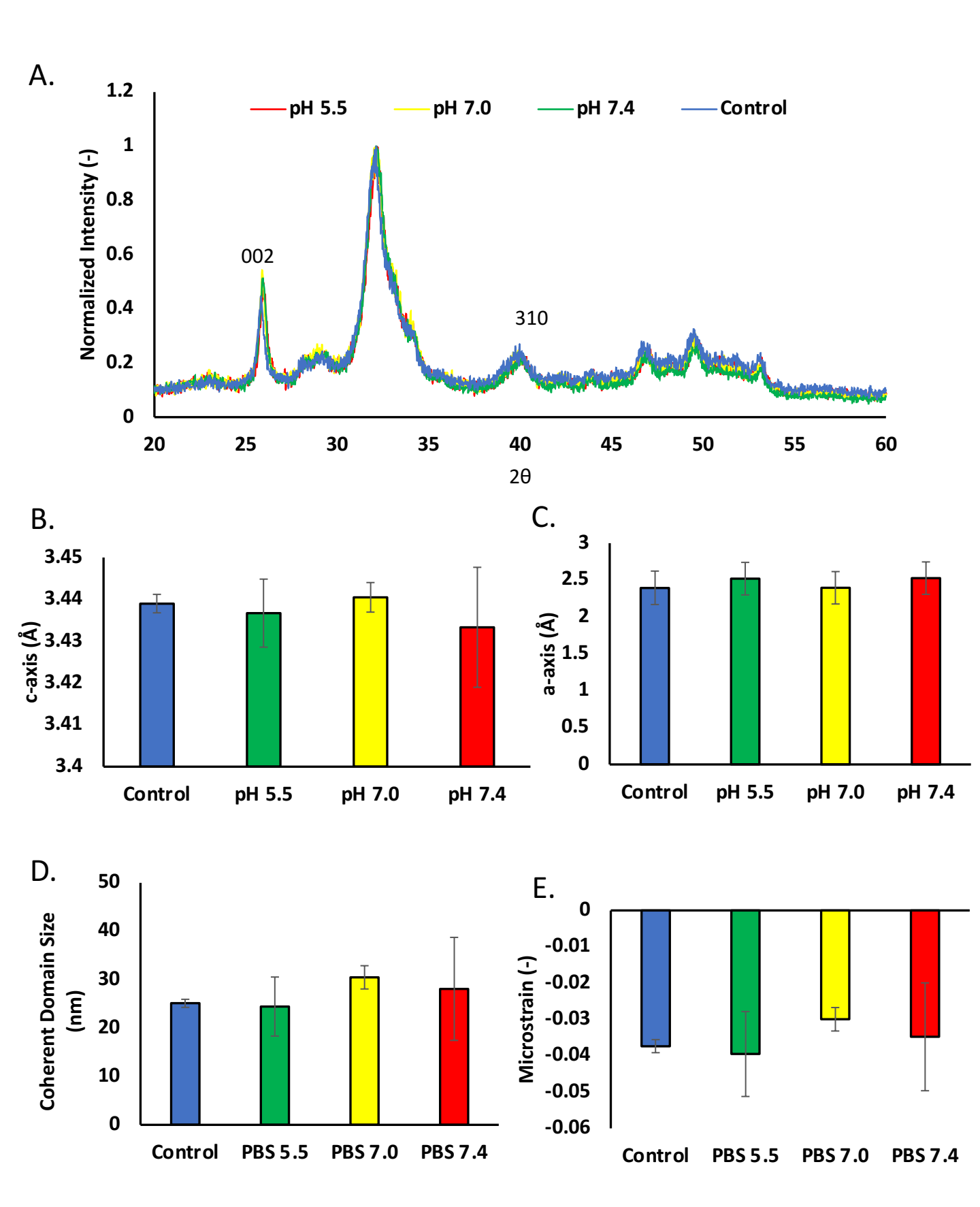


Figure 6.



Supplemental Data

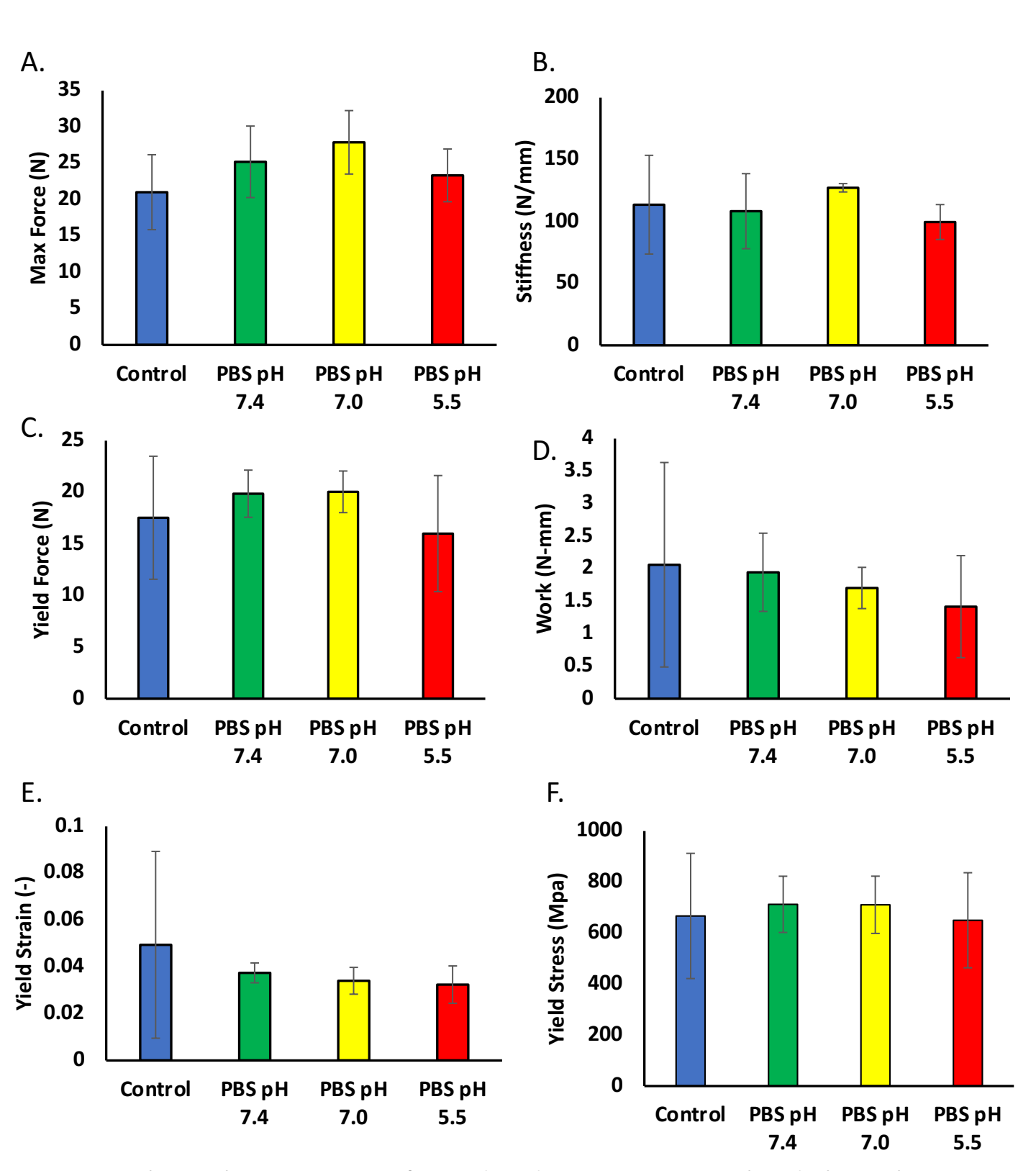
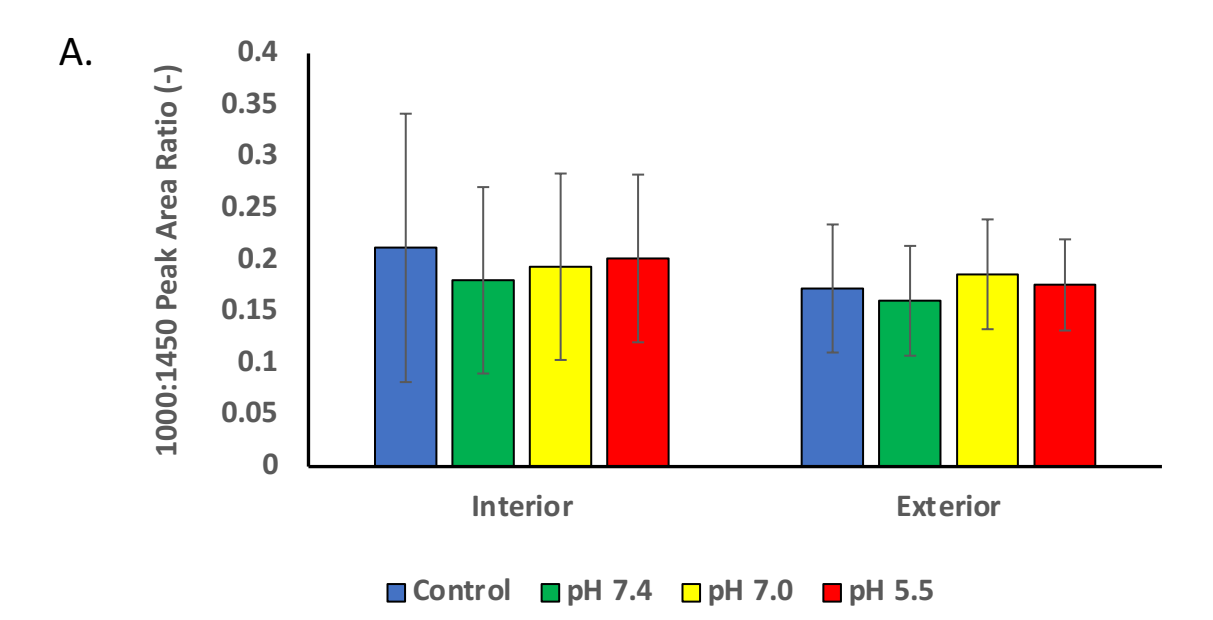


Fig 1. Mechanical tests were performed to determine material and physical properties, there was no changes in the physical properties, (A) average max force, (B) average stiffness, (C) average yield force, (D) average work, (E) average yield strain, and (F) yield stress.



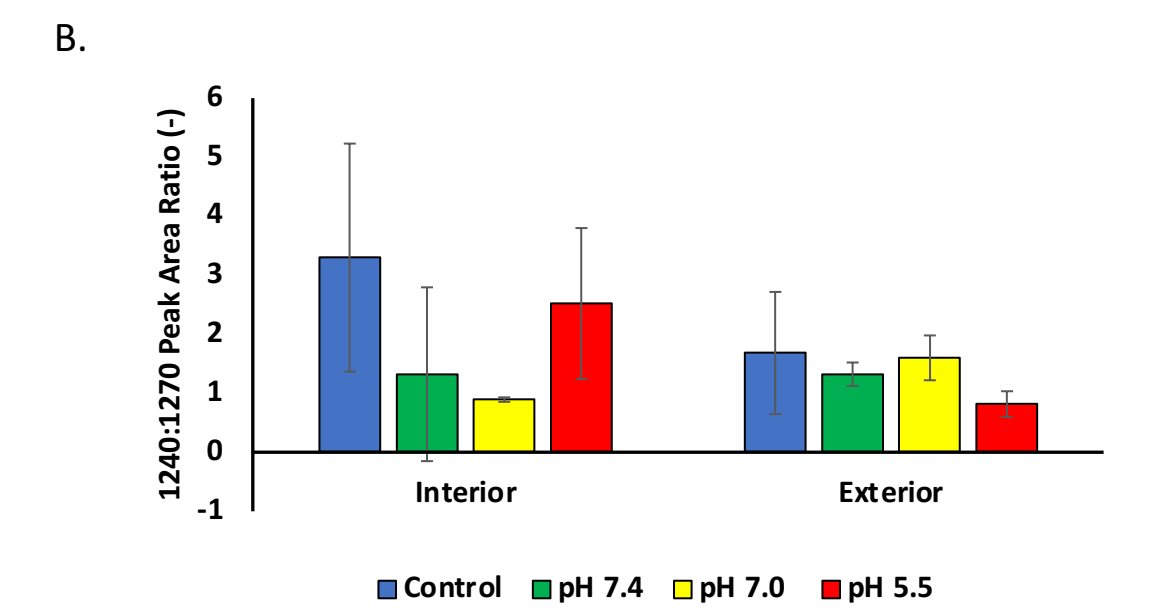


Figure 2. Raman analysis shows no changes in (A) 1000:1450 peak ratio and (B) 1240:1270 peak ratio

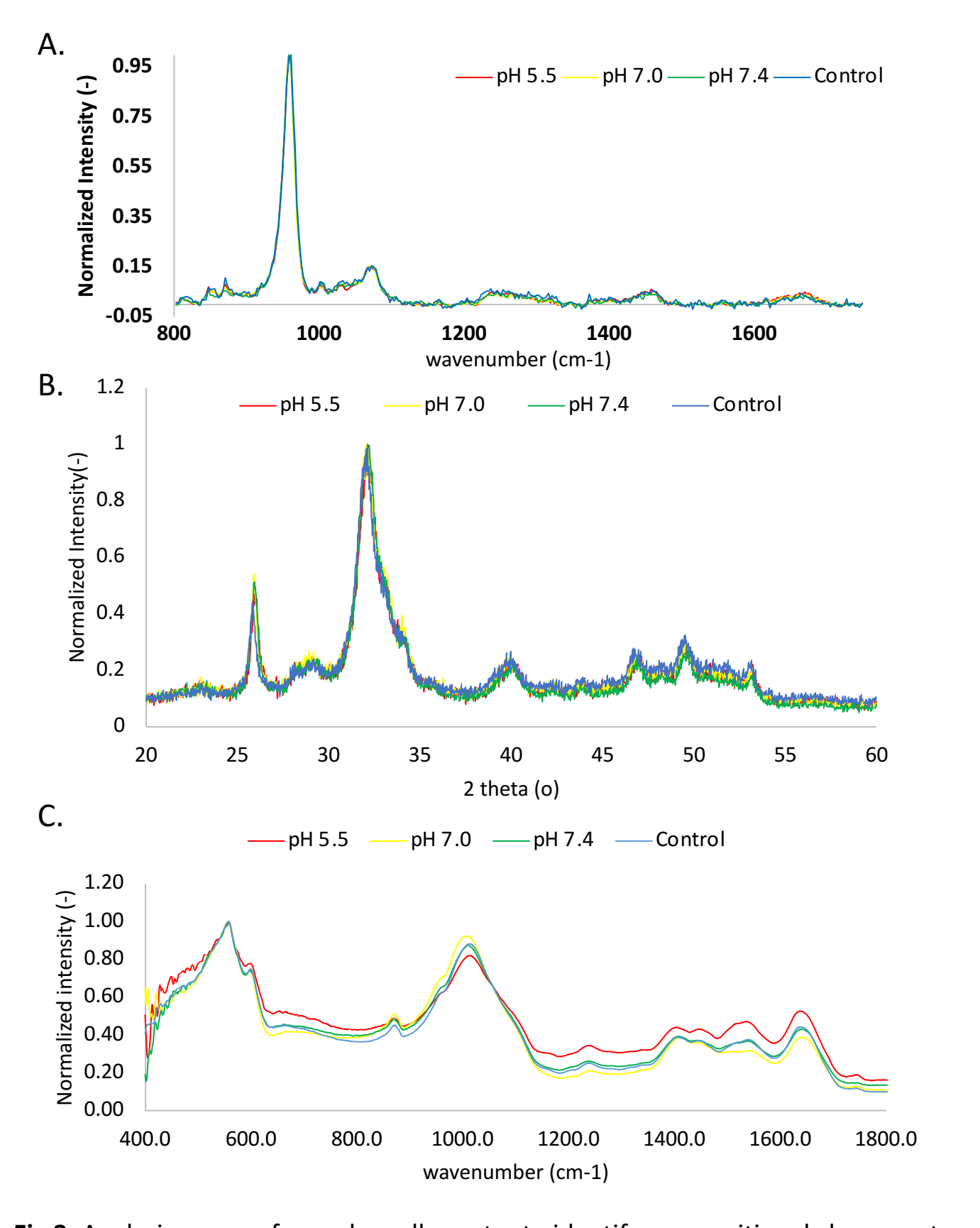


Fig 3. Analysis was performed on all spectra to identify compositional changes at different peaks. (A) Representative normalized Raman spectra from each condition, (B) Representative normalized XRD spectra from each condition, (C) Representative normalized FTIR spectra from each condition

	Initial			Max				Min:Mat	Min:Mat	1000/1660	1000/1660	1660:1450	1660:1450	1660 Width	1660 Width	1670/1640						Apatitic
	pН	рН	Toughness	Stress	Modulus	Interior	r	Interior	Exterior	Interior	Exterior	Interior	Exterior	Interior	Exterior	Interior	Exterior	Labile	Type B	Type A	HPO ₄ -	HPO ₄ -
Initial pH	1	0.99	-0.32	-0.11	0.07	-0.05	0.10	0.79	0.35	0.47	0.64	-0.74	0.17	0.01	-0.80	0.16	-0.54	0.55	-0.31	-0.42	-0.01	0.61
Final pH		1.00	-0.35	-0.13	0.06	-0.10	0.13	0.82	0.38	0.49	0.64	-0.69	0.11	-0.05	-0.79	0.10	-0.49	0.53	-0.24	-0.44	0.01	0.61
Toughness			1.00	0.71	-0.07	0.26	0.00	0.28	-0.67	-0.45	-0.11	0.23	-0.11	0.36	0.54	-0.16	0.44	0.22	0.20	-0.26	0.06	-0.58
Max Stress				1.00	0.48	0.29	-0.03	0.30	-0.28	-0.47	-0.02	0.35	0.36	-0.23	0.25	-0.31	0.18	0.48	0.09	-0.43	0.11	-0.44
Modulus					1.00	0.30	-0.11	-0.11	0.18	-0.10	-0.04	0.48	0.58	-0.71	-0.44	-0.25	-0.33	0.53	0.17	-0.50	0.25	-0.16
CO ₃ ²⁻ Interior						1.00	-0.56	-0.23	-0.34	-0.05	-0.05	-0.18	0.02	0.13	0.13	0.29	-0.13	0.51	-0.35	-0.26	-0.13	-0.10
CO ₃ ² -								0.20				0.10		0.16			0.25			0.17		
Exterior							1.00	0.30	0.36	0.32	-0.25	0.19	0.08	0.16	0.30	-0.12	0.35	-0.31	0.20	0.17	0.58	-0.09
Min:Mat Interior								1.00	0.17	0.24	0.38	-0.29	-0.09	0.12	-0.19	-0.18	0.00	0.17	0.05	-0.16	0.21	0.10
Min:Mat																						
Exterior									1.00	0.57	-0.04	-0.07	-0.07	-0.43	-0.35	-0.19	-0.22	-0.26	-0.03	0.22	0.49	0.36
1000/1660 Interior										1.00	-0.06	-0.23	-0.34	0.09	-0.28	0.36	-0.27	0.04	0.37	-0.19	0.56	0.01
IIICIIOI																						
1000/1660																						
Exterior											1.00	-0.32	-0.03	-0.15	-0.32	0.09	0.05	0.45	-0.16	-0.30	-0.42	0.63
1660:1450 Interior												1.00	0.05	-0.37	0.35	-0.37	0.38	0.01	0.46	-0.21	0.39	-0.37
interior												2.00	0.03	0.57	0.55	0.07	0.50	0.01	0.10	0.21	0.00	0.57
1660:1450																						
Exterior													1.00	-0.38	-0.32	-0.05	-0.47	0.18	-0.22	-0.05	-0.14	-0.01
1660																						
Width Interior														1.00	0.31	0.58	0.19	-0.26	-0.27	0.33	0.06	-0.02
1660																						
Width Exterior															1.00	-0.10	0.81	-0.22	0.21	0.09	0.04	-0.44
1670/1640 Interior																1.00	-0.25	0.19	-0.28	-0.03	0.05	0.21
1670/1640 Exterior																	1.00	-0.07	0.14	0.00	0.05	-0.09
Labile																		1.00	0.22	-0.90	-0.09	-0.14
Type B																			1.00	-0.61	0.33	-0.67
_																				4	0	
Type A																				1.00	-0.07	0.41
Non																						
apatitic HPO4 ⁻																					1.00	-0.25
Apatitic																						

Table 1: Correlation table showing the correlation factors relating pH, bone composition and bone mechanics.